Tectonic implications of the discovery of a Shawinigan ophiolite (Pyrites Complex) in the Adirondack Lowlands

Jeff Chiarenzelli[1,*], Marian Lupulescu[2,*], Eric Thern[3,*], and Brian Cousens[4,*]
[1]*Department of Geology, St. Lawrence University, Canton, New York 13617, USA*
[2]*New York State Museum, Research and Collections, Albany, New York 12230, USA*
[3]*Department of Imaging and Applied Physics, Curtin University of Technology, GPO Box U1987, Perth, WA 6001, Australia*
[4]*Department of Earth Sciences, Carleton University, 1125 Colonel By Drive, Ottawa, Ontario K1S 5B6, Canada*

ABSTRACT

The Pyrites Complex in the Adirondack Lowlands domain of the Grenville Province forms the core of a large NE-trending, elongate, winged structure ~15 km long dominated by highly deformed metagabbro, amphibolite, and hornblende schist. A previously unrecognized km-scale boudin of metamorphosed ultramafic rocks associated with the belt is described. It is largely replaced by secondary hydrous minerals, but retains relict igneous textures and some primary minerals such as augite and chromite, and is cut by several 1–2-m-wide lamprophyre dikes. The ultramafic rocks are interpreted as part of an obducted ophiolite complex on the basis of its structural contact with a belt of rocks including marine metasedimentary rocks, pyritic gneisses, metagabbros, and amphibolites with mid-ocean ridge basalt chemistry and were emplaced within a collapsing backarc basin of Shawinigan age. Small (50–200 µ) zircon crystals separated from peridotite and pyroxenite yield minimum ages (1140 ± 7 and 1197 ± 5 Ma) and constrain the timing of metamorphic and thermal events associated with the Shawinigan orogenesis and anorthosite-mangerite-charnockite-granite (AMCG) plutonism. Neodymium T_{DM} ages from the Pyrites Complex range from 1440 to 2650 Ma, are not compatible with derivation from a typical depleted mantle reservoir, and suggest, along with incompatible element concentrations, that these rocks record mantle enrichment, presumably during subduction beneath the leading edge of Laurentia. Rifting and development of oceanic crust between the southern Adirondack Highlands and Lowlands, coincident with a similar backarc rifting in the Central Metasedimentary Belt at ca. 1300 Ma, are proposed. Three mafic suites in the Adirondack Lowlands are distinguished by their field relations, age, geochemistry, and Nd isotopic systematics and reflect the various stages of evolution of the Trans-Adirondack backarc basin. Within the Lowlands interleaved evaporites, metasedimentary and possible metavolcanic rocks, calc-alkaline and transitional plutonic rocks, and ophiolitic rocks of the Pyrites Complex provide constraints on the tectonic processes and sedimentary response to development of a backarc basin, magmatic arc, foredeep sedimentation, and ophiolite obduction during Shawinigan convergence from ca. 1200–1160 Ma, which culminated in slab breakoff and plate delamination resulting in intrusion of the AMCG suite throughout the Frontenac-Adirondack terrane and beyond.

INTRODUCTION

During the assembly of Rodinia, large parts of the Grenville Province (Fig. 1; Rivers, 1997), including the Adirondack Mountains of New York, underwent three distinct tectonic events over more than 350 m.y. (ca. 1350–1000 Ma; Elzevirian, Shawinigan, and Grenvillian orogenies of Rivers, 2008). However, even within a relatively small portion of the orogen such as the Adirondacks, the extent and nature of these events varies significantly (Heumann et al., 2006; Bickford et al., 2008). Defining and understanding the tectonic context of regional metamorphism, the nature of the boundaries and relative motion along them, and the tectonic events that caused them, are major challenges in the Adirondacks, the Grenville Province, and deeply exhumed orogens worldwide. Furthermore, advances in our understanding of the Grenville Province are critical to facilitate our interpretation of the deep crustal architecture of orogenic belts worldwide (Rivers, 2008), the assembly of supercontinents, and temporal changes in tectonic processes.

One of the most fundamental boundaries in the Adirondacks is the Carthage-Colton shear zone (Fig. 2), which separates Grenvillian rocks of the Central Metasedimentary Belt (Adirondack Lowlands) from those of the Central Granulite terrane (Adirondack Highlands). In contrast to the Highlands, and despite many similarities, the Lowlands have a recognized stratigraphy and greater volume of supracrustal rocks (80%–85%; Carl and deLorraine, 1997), lower metamorphic grade, different structural style and grain, and lack widespread (any?) Ottawan deformation and thermal overprint and magmatism related to the Lyon Mountain Granite suite (however, see the monazite results of Hudson et al., 2004, Dahl et al., 2005, and Hudson et al., 2008). These differences have been attributed to variations in crustal level during tectonism, prior to orogenic collapse manifested by downdropping of the Lowlands along the Carthage-Colton shear zone (McLelland et al., 1996; Selleck et al., 2005). Selleck et al. (2005) have confirmed the Carthage-Colton shear zone's role in extensional orogenic collapse and channeling of late to post-tectonic leucogranites (Lyon Mountain Granite) during the late Ottawan phase of the Grenvillian orogeny (1090–1020 Ma; Rivers, 2008); however, its earlier history is less well constrained, although differences in metamorphic grade and geochronology have been documented (Mezger et al., 1992; Streepy et al., 2001).

Radiometric ages and isotopic data, underpinned by field and structural studies in the Lowlands and contiguous portions of the Grenville Province, have provided constraints by which possible tectonic models for the southern Grenville Province can now be more fully evaluated (McLelland et al., 1996; Hanmer et al., 2000;

*Emails: Chiarenzelli: jchiaren@stlawu.edu; Lupulescu: mlupules@mail.nysed.gov; Thern: eric@thern.org; Cousens: bcousens@earthsci.carleton.ca.

Geosphere; April 2011; v. 7; no. 2; p. 333–356; doi: 10.1130/GES00608.1; 17 figures; 8 tables.

For permission to copy, contact editing@geosociety.org
© 2011 Geological Society of America

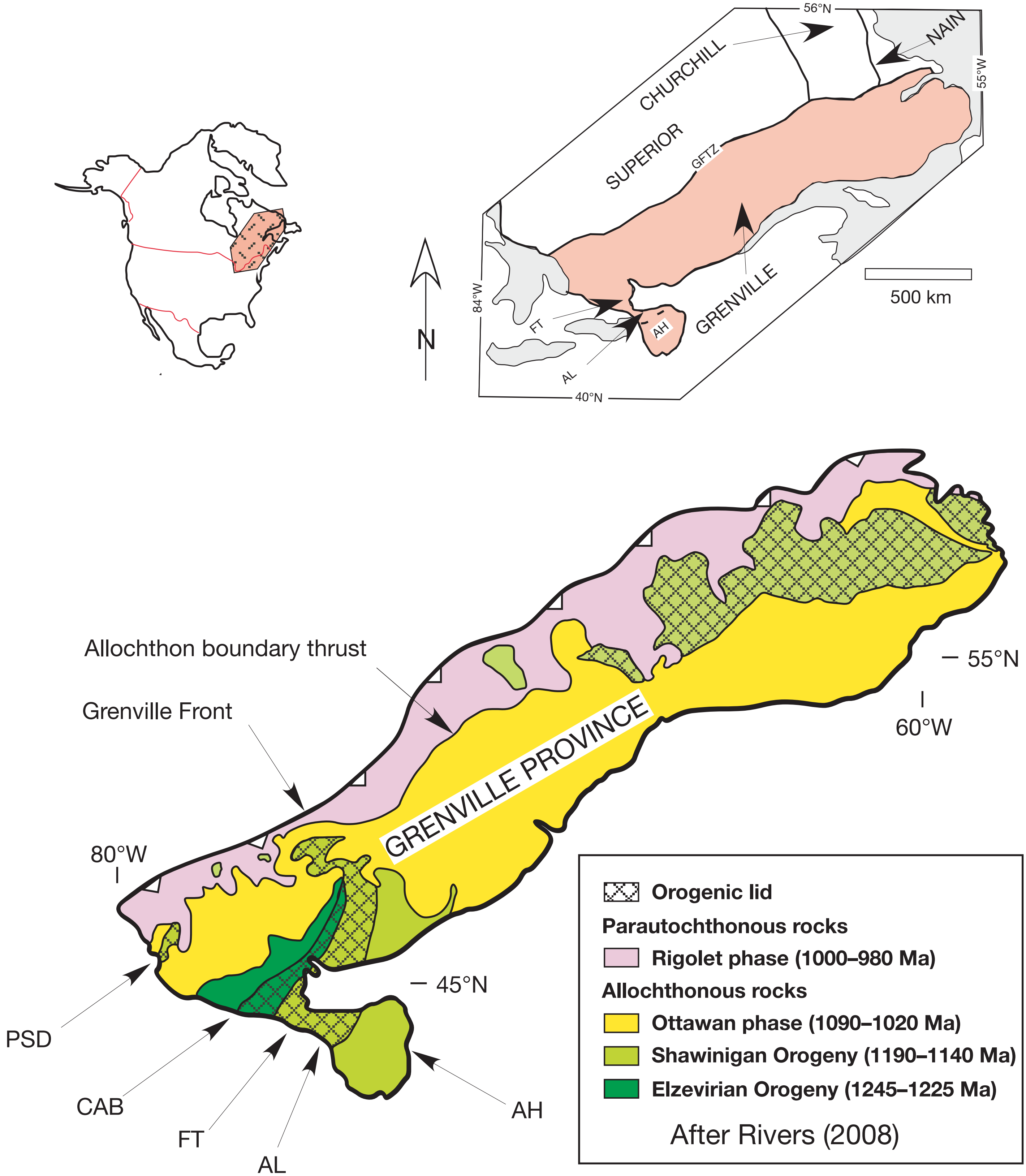

Figure 1. General location diagram showing subdivisions of the Grenville Province after McLelland et al. (1996), Rivers (1997), and Rivers (2008). Upper diagram: AH—Adirondack Highlands; AL—Adirondack Lowlands; FT—Frontenac Terrane; GFTZ—Grenville Front Tectonic Zone. Lower diagram: AH—Adirondack Highlands; AL—Adirondack Lowlands; CAB—Composite Arc Belt; FT—Frontenac Terrane; PSD—Parry Sound domain. Inset shows location of the Grenville Province with respect to North America.

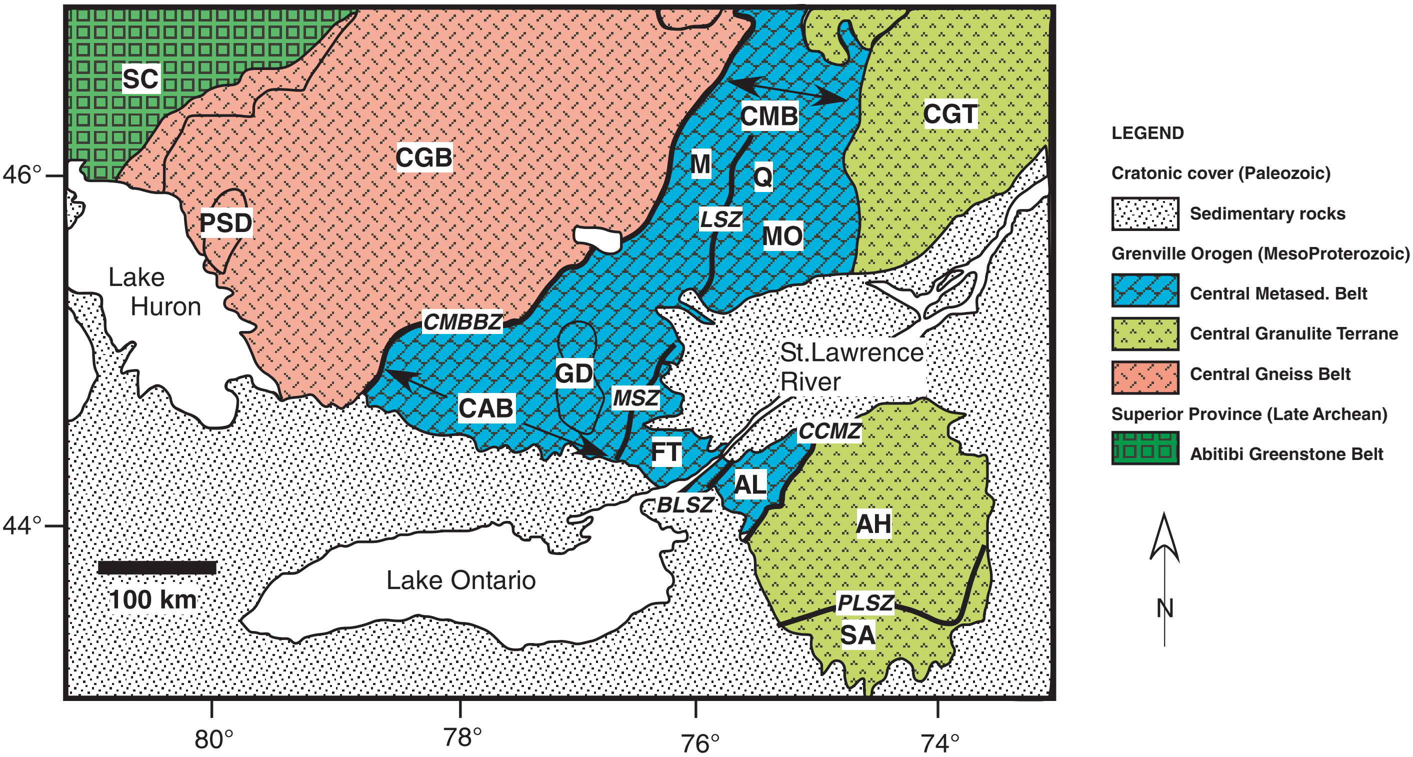

Figure 2. A location map displaying the tectonic subdivisions and major structures of the southwest Grenville Province and Adirondack dome (modified from McLelland et al., 2010; Dickin and McNutt, 2007; Rivers, 2008). Terranes and domains: AH—Adirondack Highlands; AL—Adirondack Lowlands; CAB—Composite Arc Belt; CGB—Central Gneiss Belt; CGT—Central Granulite terrane; CMB—Central Metasedimentary Belt; FT—Frontenac terrane; GD—Grimsthorpe domain; M—Marble domain; MO—Morin terrane; Q—Quartzite domain; PSD—Parry Sound domain; SA—Southern Adirondacks; SC—Superior craton. Major structures: *BLSZ*—Black Lake shear zone; *CCMZ*—Carthage Colton mylonite zone; *CMBBZ*—Central Metasedimentary Belt boundary zone; *LSZ*—Labele shear zone; *MSZ*—Maberly shear zone; *PLSZ*—Piseco Lake shear zone.

Rivers, 2008; McLelland et al., 2010). Given the general lack of pervasive Ottawan deformation and associated granulite-facies metamorphism, the Lowlands provide a rare window into the Shawinigan orogeny where original stratigraphic relations are at least partially preserved. Despite this, rocks of Adirondack Lowlands and the contiguous Canadian portion of Frontenac terrane are complexly deformed and metamorphosed at high grade, and the new data described herein provide additional constraints that can be incorporated into future discussions and models.

Southeast Laurentia is believed to have been a long-lived Andean-style margin developed above NW-directed subduction zones (Carr et al., 2000; Hanmer et al., 2000; Rivers and Corrigan, 2000). Proposed models include the development of a backarc basin in the Ontario-Quebec-Adirondack segment after 1300 Ma, with closure of the basin and associated tectonism at ca. 1200 Ma. Based on Nd isotopic evidence, Dickin and McNutt (2007) recently proposed that much of the Central Metasedimentary Belt in Ontario and Quebec is a failed backarc rift zone underlain by both ensialic and ensimatic crust. Chiarenzelli et al. (2010b, this volume) propose that a similar and contemporaneous backarc basin (Trans-Adirondack Basin) existed between the Frontenac terrane and the southern Adirondacks. The mafic and ultramafic rocks described here form part of an obducted ophiolite sequence that once floored the Trans-Adirondack Basin (Chiarenzelli et al., 2010a).

Herein, the first documented occurrence of ultramafic rocks in the Adirondack Lowlands, New York, is summarized (Chiarenzelli et al., 2007; Lupulescu et al., 2008). The tectonic constraints provided by their field relations, geochemical characteristics, U-Pb zircon geochronology, and Nd T_{DM} ages are discussed. A model for the evolution of supracrustal rocks in the Lowlands prior to the Shawinigan orogeny is proposed in light of evolving models for Grenville tectonism now incorporating the occurrence of ultramafic and mafic rocks of oceanic affinity (ophiolite) in the Adirondack Lowlands.

GEOLOGICAL SETTING

The Adirondack Lowlands consist of a diverse array of metaigneous and metasedimentary rocks (Fig. 3). The lower marble, currently the oldest recognized lithologic unit in the Lowlands, consists of a diverse assemblage of calcitic marble with interlayered calc-silicates, quartzites, biotite and pelitic gneisses, and arkosic metasandstones and tourmalinites (Brown, 1988, 1989). Sillimanite-garnet ± corundum ± spinel assemblages rim some of the Hyde School Gneiss phaccoliths and have yielded metamorphic temperatures of 830–860 °C, substantially above reported regional metamorphic temperatures (McLelland et al., 1991; Hudson and Dahl, 1998). These rocks, once considered a base to the Lowlands metasedimentary sequence, have been reinterpreted as a contact metamorphic zone associated with the intrusion of the Hyde School Gneiss at ca. 1172 Ma (McLelland et al., 1991). Marbles, volumetrically significant in the Lowlands, are also found widely throughout Central Metasedimentary Belt and Adirondack

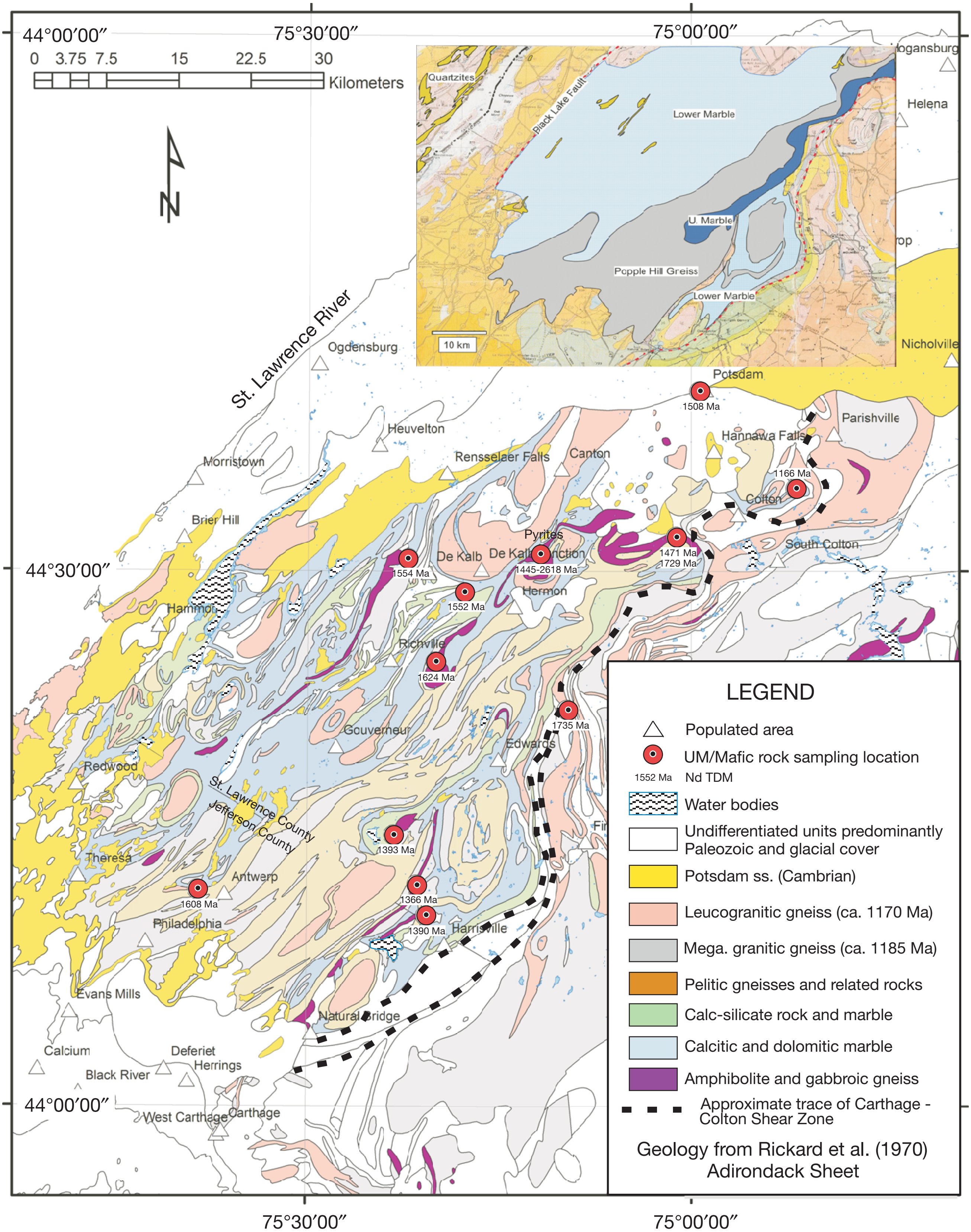

Figure 3. Simplified geologic map of the Adirondack Lowlands after the Adirondack sheet 1:250,000 (Rickard et al., 1970). Circles show locations and place names of samples discussed in text. Inset shows the generalized distribution of metasedimentary lithologic units in the Lowlands superimposed on a scanned portion of the Adirondack sheet of Rickard et al. (1970).

Highlands (McLelland and Isachsen, 1986; Easton, 1992; deLorraine and Sangster, 1997), but correlation across this wide area is unlikely due to structural complexities and distances.

The Popple Hill Gneiss overlies the lower marble and consists of a wide variety of lithologies including pelitic and pssamitic gneisses containing primarily quartz-biotite-plagioclase–K-feldspar. Locally, the Popple Hill Gneiss contains large proportions of garnet and/or sillimanite and anatectic melt. Its overall composition is highly variable and has been described as dacitic by Carl (1988); and it represents a partially melted and highly metamorphosed shale-sand sequence with possible volcaniclastic input. In some areas it is extensively migmatized and in others contains numerous (up to 100-m-thick) concordant amphibolitic layers interpreted as sills and/or dikes of basaltic composition (Carl, 2000). Zircons separated from the Popple Hill Gneiss from locations throughout the Adirondack Lowlands and Highlands yield zircon populations indicating anatexis at 1180–1160 Ma in the Lowlands and Highlands (Heumann et al., 2006), as well as 1080–1040 Ma in the eastern Highlands (Bickford et al., 2008). Zircons, interpreted as detrital cores, yield ages as young as ca. 1220 Ma, constraining the maximum age of at least part of the Popple Hill Gneiss and overlying upper marble.

Because it hosts the Balmat sphalerite and talc deposits, the stratigraphy of the upper marble is well characterized by hundreds of drill cores that have penetrated the Sylvia Lake syncline. It is the uppermost unit in the Lowlands and has been subdivided into 16 units consisting primarily of pure and silicated dolomitic marbles (deLorraine and Sangster, 1997). Other units include anhydrite, talc-tremolite-cummingtonite schist, and pyritic pelitic schists. Unit 4 is noteworthy for the presence of possible overturned stromatolites on the recumbent limb of the Sylvia Lake syncline. Deposition in shallow, marine conditions with abundant algal life is supported by the presence of natural gas discovered during drilling related to initial sphalerite exploration efforts (Brown, 1932) and the occurrence of widespread "fetid" marbles in both the upper and lower marbles.

In addition to the aforementioned lithologies, a wide variety of amphibolitic and metagabbroic units of uncertain origin are found throughout the Lowlands (Carl, 2000). Some are clearly intrusive and display igneous textures and plutonic contacts, and are best considered metagabbros or metadiorites. Many of these may be mafic equivalents of the Antwerp-Rossie plutonic suite. Others are strongly deformed and highly disrupted and intruded by granitic to tonalitic members of the Antwerp-Rossie suite and thus have a minimum age of ca. 1200 Ma (Wasteneys et al., 1999; Chiarenzelli et al., 2010b). Still others are intimately associated with thin, pyritic gneiss units that can be traced for over 50 km or more in NE-trending belts in the Lowlands that were mined for sulfur in the late 1800s and early 1900s (Prucha, 1957). In the Colton-Pierrepont area (Fig. 3), amphibolites appear to extensively intrude rocks of the Popple Hill Gneiss and lower marble (Tyler, 1979) in accord with our own observations.

Several intrusive suites are known throughout the area and intrude the metasedimentary sequence noted above (Carl and deLorraine, 1997). These include the Antwerp-Rossie suite intruded at ca. 1200 Ma (Wasteneys et al., 1999; Chiarenzelli et al., 2010b), the Hermon granitic gneiss (1182 ± 7 Ma; Heumann et al., 2006), and the Hyde School Gneiss (ca. 1172; Wasteneys et al., 1999). The Hyde School Gneiss has a variable composition (granitic to tonalitic) and is primarily exposed in about a dozen large, elliptical domes. It and the Rockport Granite, exposed in the Frontenac terrane, may represent transitional magmatism following intrusion of the Antwerp-Rossie suite and predating initiation of the anorthosite-mangerite-charnockite-granite (AMCG) magmatism (Chiarenzelli et al., 2010b). Rocks of the AMCG suite include the Edwardsville syenite (1164 ± 4 Ma; McLelland et al., 1993). These ages and dating of zircon from leucosomes in the Popple Hill Gneiss (Heumann et al., 2006) indicate high-grade metamorphic conditions and deformation occurred during the peak of Shawinigan orogenesis from 1180 to 1160 Ma). Shortly thereafter, by ca. 1155 Ma, regional deformation ceased and cooling of the area began (Mezger et al., 1991; McLelland et al., 2010).

Inspection of a map of the Adirondack Lowlands (Fig. 3; Rickard et al., 1970) reveals a strong NE-trending structural grain defined by linear lithologic belts. This is particularly true for the supracrustal units but also in part for the Antwerp-Rossie suite and Hermon granitic gneiss suites. The Hyde School Gneiss, however, appear to form foliation deflecting composite plutons or structural domes originally termed phaccoliths by Buddington (1939). In addition, a progressive change in metasedimentary rock type is apparent across strike. For example, larger bodies of quartzite consisting of quartzose, feldspathic, or calc-silicate–bearing metamorphosed sandstones are generally restricted to the area NW of the Black Lake shear zone. Farther to the SE they give way to the lower marble, then the Popple Hill Gneiss, and then the upper marble. Near the Carthage-Colton shear zone the lower marble reappears, suggesting that it extends underneath the Popple Hill Gneiss and upper marble. Plutons of the Antwerp-Rossie suite are located primarily within the northwest portion of the lower marble belt, while the Hermon granitic gneiss extensively intrudes the Popple Hill Gneiss belt, also showing a strongly linear outcrop pattern, consistent with emplacement as intrusive sheets (Fig. 3). Rocks of the Hyde School Gneiss suite are found across the entire region, and correlative felsic plutons of the Rockport Granite are found west of the Black Lake shear zone and across the Frontenac terrane (Marcantonio et al., 1990).

The rocks in the Lowlands have undergone extensive deformation and metamorphism to upper amphibolite facies resulting in partial melting and zircon growth in pelitic gneisses (Heumann et al., 2006). DeLorraine and Sangster (1997) note that rocks in the Balmat Mine have undergone four phases of deformation. Early structures include intrafolial, isoclinal folds that deform compositional layering interpreted as bedding where it is concordant to major lithologic units. These isoclines, and the prominent axial planar foliation formed in schistose lithologies, are refolded about isoclines whose axial traces trend NE and form complex recumbent folds. Later upright, tight to open, NNE and NW folds refold earlier structures resulting in fold interference patterns.

Structural cross sections suggest steepening and tightening of large-scale Phase 2a antiforms and synforms to the southeast and continuing deformation (Phase 2b) resulting in porpoising hinges and sheath folds (deLorraine and Sangster, 1997). The overall structure is consistent with a SE-verging fold-and-thrust belt. Some authors have suggested the occurrence of NE-trending structural panels bounded by shear zones and major lineaments such as the Black Lake shear zone. However, deLorraine and Sangster (1997) conclude that major stratigraphic units cross such boundaries arguing against terrane boundaries or considerable displacement. The presence of southeast-vergent thrust sheets has been established based on the structural discontinuities, the presence of mylonitic shear zones, and the excision of stratigraphic units (deLorraine and Sangster, 1997; Hudson and Dahl, 1998). For example, the upper and lower marbles are in structural contact near Edwards, and the entire Popple Hill Gneiss section has been excised by the Elm Creek thrust (Elm Creek slide of deLorraine and Sangster, 1997). While the regional stratigraphy has been firmly established, it is disrupted and crosscut by major structures and plutonic rocks in many areas and best considered a tectonostratigraphy on the local level, unless evidence to the contrary is provided, such as in the Sylvia Lake syncline (deLorraine and Sangster, 1997).

The overall picture is one of a more or less coherent stratigraphic sequence from the Frontenac terrane across the Lowlands which has been folded and thrusted, and intruded by a diverse set of preorogenic, synorogenic, and postorogenic plutonic rocks. The belt-like, NE-trending occurrence of many of the lithologies is likely a function of their original distribution and subsequent shortening, largely perpendicular to their strike. Large-scale folds form a series of upright to inclined antiformal and synformal structures, such as the Sylvia Lake syncline. Interspersed shear zones and ductile thrusts disrupt the stratigraphy. The significance of orogen-parallel structures in the region has yet to be fully evaluated in the region, although oblique motion on the Carthage-Colton mylonite zone and other shear zones is likely (Johnson et al., 2004; Baird, 2006; Reitz and Valentino, 2006).

FIELD RELATIONSHIPS AND ANALYTICAL RESULTS

Pyrites Complex

At Pyrites, New York (Fig. 3), metamorphosed ultramafic-mafic rocks (Pyrites Complex) are in structural contact with rusty, graphite-bearing, pyritic gneisses (Fig. 4). The ultramafic lithologies occur as a large, compositional layered xenolith or core within more extensive and deformed belt of metagabbroic and amphibolitic rocks. Primary compositional layering (decimeter to meter scale) in the peridotite is discordant to the regional and local foliation trends and lithologic contacts (Fig. 5). A large (2-m-wide), undeformed, and coarse-grained (2–3 cm) phlogopite lamprophyre cuts the peridotite and its compositional layering. Layers within the peridotite include coarse (1–3 cm), knobby weathered pyroxenite (Fig. 6) and altered, massive to weakly layered peridotite. In all, ~1 km^2 of mafic and ultramafic rock is exposed (Fig. 7). While the aerial extent of the ultramafic complex is modest, the largest gravity values in St. Lawrence County extend from the outcrop of ultramafic rocks near Pyrites for ~10 km to the southwest (Fig. 8), suggesting that a considerable volume of dense rock occurs at depth (Revetta and McDermott, 2003). In addition, narrow bands of highly tectonized metagabbro, amphibolite, and hornblende schist can be traced from this central block both NE and SW for several for ~15 km. To the west, the amphibolites are associated with rusty pyritic gneisses mined extensively for sulfur at the Stellaville mine from 1883 to 1921 (Prucha,

Figure 4. Photograph looking south showing the tectonic contact (thrust) between underlying strongly foliated gabbroic rocks (left side) and pyritic pelitic gneisses (right side) in the bed of the Grasse River, just south of the hydrostation at Pyrites, New York.

Figure 5. Photograph looking north showing the moderately dipping and compositionally layered ultramafic rocks of the Pyrites Complex. The exposure is in the parking lot of the hydrostation at Pyrites, New York. Field book for scale.

Figure 6. Photograph looking east showing the contact between knobby weathering pyroxenite (below) and weakly layered and sheared overlying peridotite (above) along the bank of the Grasse River at Pyrites, New York. Geologic pick for scale.

1957). Together these rocks occur as a folded layer and/or thrust sheet(s) within the lower marble (Rickard et al., 1970) and therefore must predate Shawinigan deformation in the Lowlands (ca. 1160–1200 Ma).

Samples were collected from exposures of ultramafic and mafic rocks along the Grasse River in Pyrites ~15 km northwest of the trace of the Carthage-Colton mylonite zone. The ultramafic rocks range in color from pale green to greenish black and display extensive development of magnesium-rich, hydrous, secondary minerals. For the peridotite and pyroxenite these include mixtures of tremolite, talc, serpentine, chlorite, and dolomite (Lupulescu et al., 2008) and are consistent with loss on ignition values that average ~8 wt%. The lamprophyre contains large phenocrysts of phlogopite, apatite, and secondary(?) annite, in addition to other hydrous magnesium silicates. Of the pseudomorphically replaced primary minerals (CIPW-normative olivine, orthopyroxene and clinopyroxene, chromite, and calcic plagioclase) only chromite and limited amounts of augite are preserved. On the International Union of the Geological Sciences (IUGS) ultramafic plutonic rock classification diagram, using CIPW norms (Streckeisen, 1973), they plot mostly as lherzolite but show a range in composition, some of which may be due to alteration (Fig. 9). The large relic grain size, textures, and decimeter-scale layering confirm an original variation in composition. Accessory minerals include magnetite, ilmenite, chromite, apatite, and trace amounts of titanite, zircon, and rutile. Geochemically the rocks range from 33.74 (phlogopite lamprophyre) to 52.09 (metagabbro) wt% SiO_2, with ultramafic cumulate rocks containing 25–33 wt% MgO and up to 5440 ppm Cr and 1588 ppm Ni (Table 1). In addition, the rocks are characterized by low (<1.0 wt%) TiO_2.

Routine petrographic and scanning electron microscopy (SEM) investigation revealed the occurrence of small (50–200 micron) zircon crystals in some of the ultramafic rock (Figs. 10 and 11). Zircon grains were separated by standard techniques and purified by handpicking prior to mounting in epoxy for cathodoluminescence (CL), sensitive high-resolution ion microprobe (SHRIMP), and laser ablation–inductively coupled plasma–mass spectrometry (LA-ICP-MS) analysis. Sensitive high-resolution ion microprobe analyses were carried out at the John De Laeter Center for Isotope Research in Perth, Australia, and procedures followed the methods of Nelson (1997). Laser ablation ICP-MS analyses were carried out at the Arizona Laserchron Center in Tucson, Arizona, and methods are published on the web (http://www.geo.arizona.edu/alc). Geochemical analyses were carried out by standard X-ray fluorescence (XRF), inductively coupled plasma–optical emission spectroscopy (ICP-OES) and ICP-MS techniques at GeoAnalytical Laboratory, Washington State University at Pullman and ACME Analytical Laboratories in Vancouver, British Columbia. Strontium and neodymium isotopes were measured at the Isotope Geology and Geochronology Research Facility at Carleton University, Ottawa (Cousens, 1996; Cousens et al., 2008). Carbon and oxygen isotopes from thin carbonate veins were analyzed at the Department of Atmospheric Sciences, State University of New York at Albany.

Small (50–200 µm) zircon crystals were separated from a peridotite sample containing 41.59 wt% SiO_2 and 32.07 wt% MgO. The zircon grains have anhedral to faceted shapes and display fine and sector zoning in CL (Fig. 11). No evidence of cores or metamorphic rims was visible. The grains averaged 408 ± 91 ppm U and have Th/U ratios of 0.27 ± 0.03 (Table 2). Sensitive high-resolution ion microprobe (SHRIMP) II analyses (Fig. 12; Table 2) yielded two age groups—1202 ± 20 Ma (2σ, n = 2) and 1140 ± 7 Ma (2σ, n = 20). Zircon of similar morphology and size discovered embedded in serpentine, replacing a knobby weathering pyroxenite (38.48 wt. % SiO_2 and 33.33 wt. % MgO), yielded a U-Pb LA-ICP-MS age of 1197 ± 5 Ma (2σ, n = 43; Fig. 13; Table 3). The zircons averaged 460 ± 296 ppm U and have Th/U ratios of 0.55 ± 0.33. Four grains were discordant and are not shown on Figure 13; a fifth grain yields a nearly concordant age of 558 ± 38 Ma.

Samples of mafic and ultramafic rocks, all collected along the banks of the Grasse River in Pyrites, were analyzed for Rb-Sr and Sm-Nd isotopic systematics at the Department of Earth Sciences, Carleton University (Fig. 14; Tables 4 and 5). Neodymium T_{DM} ages have been calculated from seven samples of mafic-ultramafic rocks and range between 1450 and 2620 Ma. Calcite samples from three thin (<5 mm) and

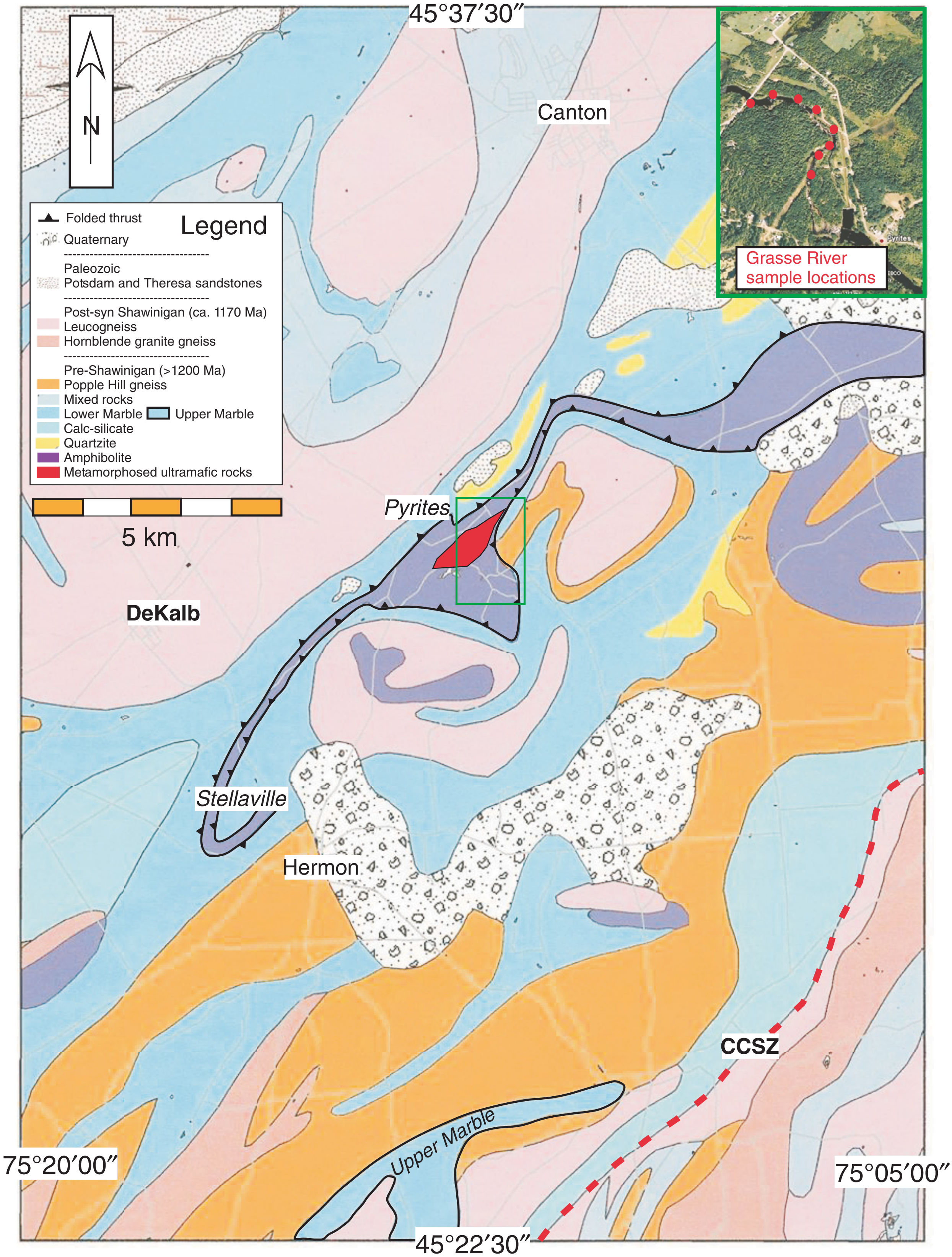

Figure 7. Geologic map of the Pyrites area modified after Rickard et al. (1970). Place names mentioned in text and roadways are shown for reference. Pyrite was mined at Pyrites and Stellaville. CCSZ—Carthage-Colton shear zone. Inset is a Google Earth image of the Grasse River at Pyrites with sample localities shown.

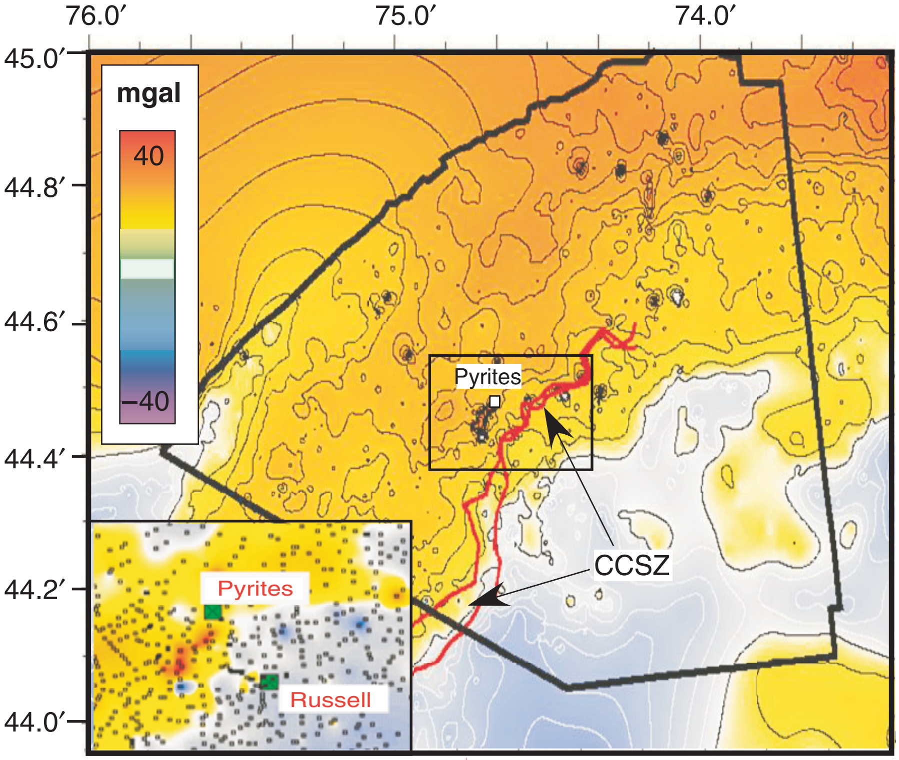

Figure 8. Gravity anomaly map centered on St. Lawrence County, New York, and showing surrounding regions of the northwestern portion of New York State. Note the linear gravity high with closely spaced contours extending SW from Pyrites, New York (circled). This area has the highest gravity values measured in St. Lawrence County. The Carthage-Colton shear zone (CCSZ) is shown for reference. Inset at twice the scale shows the location of data points collected in the immediate area. After Revetta and McDermott (2003).

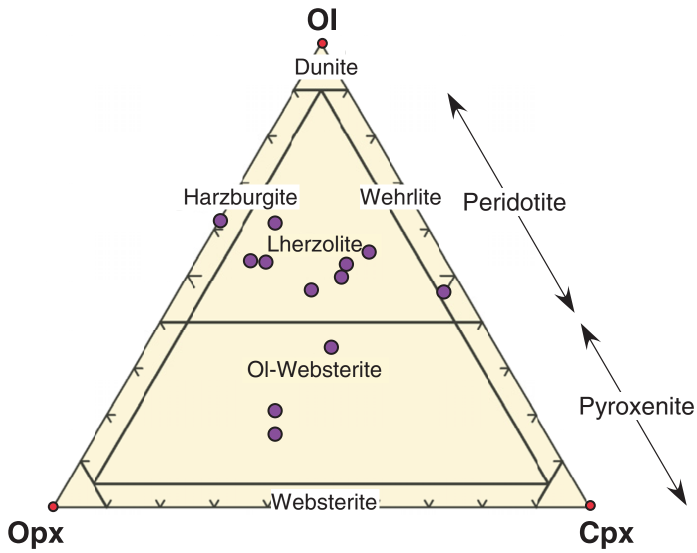

Figure 9. Classification diagram (orthopyroxene [opx]-olivine [ol]-clinopyroxene [cpx]) of the International Union of Geological Sciences (IUGS) for ultramafic plutonic rocks (Streckeisen, 1973). Circles represent normalized mineralogical composition of ultramafic rocks (>90% normative mafic minerals) of the Pyrites Complex determined by calculating CIPW norms.

undeformed carbonate veins cutting the peridotite and hosting small metamorphic zircons were analyzed for carbon and oxygen isotopic composition at the Department of Atmospheric Sciences, State University of New York at Albany. They yield $\delta^{13}C_{PDB}$ values between –6.975 and –7.358 and $\delta^{18}O_{SMOW}$ values between 15.629 and 15.668 (Table 6; $^{87}Sr/^{86}Sr$ = 0.708891–0.709748).

Amphibolites and Metagabbros of the Lowlands

Numerous amphibolitic to metagabbroic rocks occur throughout the Lowlands primarily in elongate NE-trending belts (Fig. 3). While amphibolitic lithologies dominate, hornblendic schists, hornblendite, and coarser-grained metagabbroic variants also occur. These belts are structurally complex, highly disrupted and intruded by granitic to tonalitic rocks of the Antwerp-Rossie, Hermon granitic gneiss, Hyde School Gneiss, and AMCG suites. These crosscutting relationships indicate they are at least 1200 Ma old, but because of their tectonized contacts with surrounding supracrustal units, there are few constraints on their maximum age. However, they may well be the oldest rocks in the Lowlands. A wide variety of other mafic rocks, primarily occurring as small plutons or dikes, has been discussed by Carl (2000). Many of these occur as concordant layers in the Popple Hill Gneiss (up to 100 m wide) and the Hyde School Gneiss. Some, such as the Balmat gabbro, intrude the sphalerite-galena–bearing rocks in upper marble sequence at Balmat. Thus field relations indicate mafic rocks are both older, and younger, than the supracrustal sequence in the Lowlands.

A dozen samples of mafic rocks in the Lowlands were sampled for geochemistry and Sm-Nd isotopic studies (Coffin, 2008). These included a variety of amphibolites and metagabbros. One metagabbro sample, the Dana Hill metagabbro (Johnson et al., 2004), was taken just east of the Carthage-Colton shear zone in the Highlands. Three samples were taken in the Balmat area, while two were taken from sequences that included pyritic gneisses at Stellaville and Antwerp. A sample was also collected from clinopyroxene-bearing, thinly banded, amphibolite at Seven Springs, near Colton, New York. Likely a metasedimentary or volcaniclastic rock, it is intruded by a coarse-grained, K-spar augen, Hermon-type, granitic gneiss, and it structurally underlies carbonate rocks of the upper marble. Two samples were collected from the Pierrepont sigmoidal structure, a large, thick, S-shaped belt of amphibolite near the Carthage-Colton shear zone (Fig. 3). The geochemistry and location of

TABLE 1. WHOLE-ROCK GEOCHEMISTRY OF ROCKS OF THE PYRITES COMPLEX DETERMINED BY ICP-OES (MAJORS) AND ICP-MS (TRACE)

SAMPLES		PGAB	PLAMP	P06-4	P06-7	P06-8	PERID	LUP PY-A	LUP PY-K	LUP PY-B	LUP PO7-2
Lithology		GN	LM	UML	GN	GN	UML	GN	UML	UML	UML
SiO_2	(%)	52.09	33.74	39.47	48.9	49.44	41.59	40.46	40.28	40.34	41.00
TiO_2	(%)	0.63	1.57	0.35	0.84	0.58	0.11	1.79	0.24	0.19	0.26
Al_2O_3	(%)	8.38	13.8	4.56	11.09	11.44	6.61	16.88	4.12	3.70	4.48
Fe_2O_3	(%)	7.97	16.78	6.57	9.38	9.27	6.29	11.63	7.67	7.46	7.21
MnO	(%)	0.12	0.13	0.13	0.16	0.16	0.04	0.12	0.15	0.17	0.13
MgO	(%)	15.22	20.46	27.1	14.67	13.5	32.07	12.37	27.11	30.84	27.37
CaO	(%)	8.66	1.13	7.58	6.81	8.23	1.27	1.05	6.75	3.60	6.95
K_2O	(%)	2.14	2.82	0.49	2.03	1.39	1.64	6.90	0.55	0.58	0.52
Na_2O	(%)	0.53	0.03	0.36	1.4	1.88	0.26	0.06	0.47	0.33	0.62
P_2O_5	(%)	0.48	0.52	0.17	0.42	0.07	0.08	0.59	0.26	0.34	0.40
S	(%)	0.24	0.19	0.04	0.12	0.21	0.11	0.04	0.04	0.12	0.00
LOI	(%)	3.4	8.8	12.5	4.1	3.8	9.8	5.96	11.13	10.49	9.69
SUM	(%)	99.85	99.85	99.88	99.97	99.84	99.94	97.86	98.77	98.16	98.66
Mg #		0.66	0.55	0.80	0.61	0.59	0.84	0.52	0.78	0.81	0.79
Ti	(ppm)	3776	9411	2098	5035	3477	659	10755	1412	1128	1579
P	(ppm)	2096	2270	742	1834	306	349	2597	1138	1485	1766
Cr	(ppm)	1451	253	3681	985	390	376	23	3367	3249	2961
Ga	(ppm)	11.4	19.5	5.3	16.5	14.8	8.6	19	6	6	7
Ni	(ppm)	191	220	483	166	103	488	60	782	994	685
Rb	(ppm)	76.7	121.1	14.5	54.8	27.1	68.3	199.33	14.46	18.65	16.25
Sr	(ppm)	119.1	23.2	172.1	167.9	169.1	81.4	122.31	186.73	155.33	246.81
Cs	(ppm)	2.7	6.5	0.8	1.7	0.9	4.3	7.54	0.84	1.08	0.58
Ba	(ppm)	632	945.9	159.4	694.7	547.3	539	2396.04	163.24	234.32	93.23
Sc	(ppm)	46	43	44	31	45	7	14.44	25.82	18.93	37.01
V	(ppm)	200	311	117	189	226	55	257	99	88	101
Ta	(ppm)	0.1	0.5	0.1	0.4	0.1	0.7	0.37	0.07	0.07	0.19
Nb	(ppm)	2.9	8.7	1.2	8.2	1.8	3.2	7.74	1.47	1.29	3.82
Zr	(ppm)	107.1	229.9	61.2	136	87.1	59	192.93	86.20	78.06	220.33
Hf	(ppm)	3.2	7.5	1.9	4.3	3.4	2.1	5.53	2.01	1.80	5.64
Th	(ppm)	8.4	6.1	3	2.5	2.4	29.4	7.89	8.00	8.23	8.95
U	(ppm)	2.3	2	0.8	1.7	0.9	2.6	2.01	2.63	2.44	2.81
Pb	(ppm)	2	1.7	1.3	8.3	13	2.5	1.42	3.05	2.86	7.89
Cu	(ppm)	54.7	2.2	19.6	18.8	43.7	17	2	2	15	39
Zn	(ppm)	104	93	47	62	149	27	104	65	76	59
Y	(ppm)	39.9	23.7	16	31.1	24.2	7.5	14.03	21.24	19.04	27.39
La	(ppm)	22.9	7.8	26.1	33.4	14.2	105.4	10.76	30.55	22.93	42.83
Ce	(ppm)	68.5	30.1	66.3	86.4	37.3	187.3	29.37	80.83	61.48	103.53
Pr	(ppm)	12.69	6.2	10.04	12.58	5.88	17.3	4.26	11.74	9.10	15.08
Nd	(ppm)	69.9	35.6	46.3	56.3	27.9	56.8	18.26	52.03	41.26	66.68
Sm	(ppm)	19.27	9.43	10	11.53	7.1	6.4	3.85	12.10	9.67	15.31
Eu	(ppm)	4.87	1.84	2.35	2.36	1.7	1.08	0.83	3.04	2.28	3.62
Gd	(ppm)	16.69	8.09	7.56	9.55	6.27	2.97	3.25	9.97	8.24	12.64
Tb	(ppm)	2.21	1.23	0.99	1.36	1.02	0.31	0.49	1.16	0.98	1.48
Dy	(ppm)	9.74	6.24	4.29	6.52	5.01	1.38	2.86	5.16	4.58	6.68
Ho	(ppm)	1.2	0.91	0.51	0.98	0.77	0.22	0.59	0.81	0.71	1.06
Er	(ppm)	3.13	2.71	1.25	2.9	2.17	0.72	1.75	1.72	1.58	2.28
Tm	(ppm)	0.38	0.4	0.16	0.37	0.3	0.13	0.27	0.21	0.19	0.29
Yb	(ppm)	2.08	2.48	0.92	2.44	1.88	0.76	1.80	1.14	1.04	1.53
Lu	(ppm)	0.29	0.36	0.12	0.36	0.29	0.09	0.28	0.17	0.15	0.22
Th/Ta		84	12	30	6	24	42	21	109	121	48
La/Yb		11	3	28	14	8	139	6	27	22	28

Note: ICP-OES—inductively coupled plasma–optical emission spectroscopy; ICP-MS—inductively coupled plasma–mass spectrometry; LOI—loss on ignition; GN—gabbronorite; LM—lamprophyre; UML—lherzolite.

(*continued*)

these samples are given in Table 7. These samples of amphibolitic-metagabbroic rocks from throughout the Adirondack Lowlands and the Dana Hill metagabbro yield Nd T_{DM} model ages that range between 1740 and 1170 Ma.

DISCUSSION

Origin and Emplacement of the Pyrites Complex

Ultramafic rocks are found in several different settings. We suggest that the ultramafic rocks described here are most likely to have been tectonically derived from the mantle beneath or adjacent to a collapsing backarc basin. Their geological association (metabasalts and gabbros, marine metasedimentary rocks, sulfide-rich ores, and metachert-pelitic gneisses), structural emplacement rather than intrusive relationships, extensive hydrothermal alteration, enriched geochemistry and Nd systematics, and association with crosscutting lamprophyre rule out an intrusive origin. The possibility exists that they were juxtaposed with high-grade gneisses after metamorphism because they retain their hydrous nature and low-medium grade mineral assemblages; however, it is also plausible that they represent a core region that was never dehydrated despite metamorphism.

The Pyrites Complex contains a variety of ultramafic rocks, presumably of mantle affinity (Fig. 9), as well as, lamprophyre dikes. However, spidergrams of rare-earth element (REE) patterns and incompatible elements from both ultramafic and mafic samples display strong enrichment in REE and large-ion lithophile elements (LILE), and relative depletion in high field strength elements (HSFE) such as Nb, Ta, Ti, and Zr when compared to chondrites and primitive mantle (Fig. 15). Patterns are strikingly similar to those of ultrapotassic rocks derived from metasomatized mantle spanning the Snowbird tectonic zone in the Churchill Province of subarctic Canada (Cousens et al.,

TABLE 1. WHOLE-ROCK GEOCHEMISTRY OF ROCKS OF THE PYRITES COMPLEX DETERMINED BY ICP-OES (MAJORS) AND ICP-MS (TRACE) (*continued*)

SAMPLES	LUP PY-J	LUP PY-2-1	LUP PY-11	LUP P07-5	LUP P07-4	LUP PY-4	LUP P07-3	LUP PY-2A	LUP PY-1A	LUP PY-1	LUP PY-2-2
Lithology	UML	T	W	UMW	LT	UML	UML	UML	UML	UMH	GN
SiO_2	39.72	40.58	45.54	38.48	42.66	41.48	43.16	43.47	38.57	39.17	42.45
TiO_2	0.36	0.38	0.65	0.25	1.65	0.38	0.41	0.57	0.22	0.25	0.66
Al_2O_3	11.66	5.61	7.21	2.93	18.88	4.02	5.05	5.57	3.19	3.33	6.61
Fe_2O_3	4.51	6.80	6.73	8.70	12.61	7.56	6.18	5.45	8.49	8.87	5.98
MnO	0.08	0.12	0.09	0.16	0.16	0.12	0.10	0.08	0.17	0.17	0.10
MgO	26.71	24.90	21.27	33.33	6.17	29.63	27.10	22.91	31.59	32.81	19.92
CaO	6.88	8.80	8.07	1.24	9.23	3.88	6.51	10.58	3.27	1.50	13.06
K_2O	0.46	1.01	1.82	0.88	2.51	1.18	0.93	1.39	0.62	0.90	0.66
Na_2O	1.16	0.70	0.85	0.18	2.27	0.39	0.62	0.65	0.30	0.25	1.00
P_2O_5	0.24	0.28	0.24	0.19	0.86	0.09	0.24	0.23	0.18	0.22	0.23
S	0.00	0.01	0.18	0.23	0.20	0.02	0.02	0.00	0.17	0.07	0.03
LOI	7.71	8.81	4.67	11.25	1.97	9.57	8.02	7.02	11.59	10.80	7.57
SUM	99.49	98.01	97.33	97.83	99.17	98.33	98.35	97.94	98.35	98.33	98.28
Mg #	0.86	0.79	0.76	0.79	0.33	0.80	0.81	0.81	0.79	0.79	0.77
Ti	2158	2264	3886	1517	9893	2297	2478	3402	1342	1492	3980
P	1033	1237	1067	842	3765	374	1043	1020	782	941	993
Cr	29	4012	1478	2976	19	3386	3252	4244	3289	3132	5441
Ga	16	5	7	4	24	4	6	7	4	4	9
Ni	4	1176	376	1588	4	1271	611	530	1364	1531	361
Rb	9.07	41.38	66.86	41.29	62.72	54.18	36.48	58.52	25.23	36.59	16.02
Sr	98.20	170.69	222.93	100.94	790.08	89.38	228.54	142.00	114.12	87.85	230.46
Cs	3.20	1.46	2.66	1.25	1.76	1.57	1.26	1.89	1.11	1.54	0.63
Ba	70.80	205.20	574.43	193.92	498.84	280.22	242.23	275.41	148.77	228.93	115.60
Sc	9.31	38.86	50.65	11.39	26.30	19.03	45.38	55.01	12.76	10.96	72.71
V	121	97	182	62	300	74	123	143	69	66	163
Ta	0.22	0.22	0.18	0.15	0.26	0.19	0.17	0.19	0.11	0.11	0.25
Nb	2.09	3.53	3.03	2.30	4.09	2.58	2.98	3.06	1.97	2.08	3.84
Zr	137.31	148.62	167.33	117.34	59.18	95.32	171.10	105.46	96.26	87.70	132.03
Hf	3.79	3.87	4.74	3.08	2.35	2.60	4.73	3.76	2.76	2.44	4.91
Th	2.23	7.31	5.39	2.88	1.18	4.16	3.22	2.07	3.20	3.51	6.60
U	0.52	1.93	1.95	1.14	0.38	1.60	1.08	1.00	1.38	1.10	1.39
Pb	1.70	8.64	3.30	6.83	4.58	6.51	7.17	4.73	3.20	3.89	5.57
Cu	6	46	30	6	14	10	36	23	22	22	17
Zn	68	58	68	78	115	34	75	41	61	107	52
Y	14.35	18.44	29.55	12.04	49.05	12.67	23.73	21.21	14.40	13.65	28.41
La	6.01	30.81	34.71	19.12	26.13	15.82	28.06	24.89	22.81	22.23	22.52
Ce	15.40	71.03	88.97	44.35	69.79	38.31	73.53	65.64	53.31	51.15	71.93
Pr	2.48	10.13	13.85	6.28	11.32	5.62	11.26	10.31	7.56	7.13	12.76
Nd	11.98	45.01	65.63	27.46	55.64	25.34	52.56	48.64	33.01	30.62	62.63
Sm	3.25	10.33	16.62	6.21	13.47	5.98	13.19	12.02	7.66	6.97	15.85
Eu	0.79	2.46	4.55	1.39	3.24	1.44	3.22	2.76	1.69	1.53	4.01
Gd	3.04	8.31	14.16	5.01	11.96	4.95	10.92	9.70	6.37	5.74	12.82
Tb	0.50	0.98	1.66	0.62	1.82	0.61	1.31	1.17	0.74	0.70	1.54
Dy	2.85	4.47	7.51	2.85	10.21	2.90	5.91	5.36	3.40	3.21	7.14
Ho	0.58	0.71	1.16	0.47	1.99	0.48	0.94	0.84	0.55	0.53	1.13
Er	1.58	1.58	2.42	1.05	5.08	1.12	2.02	1.81	1.19	1.18	2.48
Tm	0.24	0.20	0.29	0.13	0.69	0.14	0.24	0.22	0.14	0.15	0.31
Yb	1.48	1.10	1.50	0.72	3.97	0.81	1.29	1.23	0.82	0.82	1.68
Lu	0.23	0.16	0.22	0.11	0.56	0.12	0.19	0.18	0.12	0.12	0.24
Th/Ta	10	33	30	20	5	22	19	11	29	33	26
La/Yb	4	28	23	26	7	20	22	20	28	27	13

Note: GN—Gabbronorite; LT—Leucotroctolite; T—Troctolite; UMH—Harzburgite; UML—Lherzolite; W—Websterite; based on IUGS cation normative calculations.

2001; Chiarenzelli et al., 2010a). Disturbance of both Sm-Nd and Rb-Sr isotopic systems is shown by errorchrons that yield large errors, even when the most distributed and noncollinear samples are excluded (Fig. 14). Other indicators of isotopic alteration include an initial $^{87}Sr/^{86}Sr$ ratio of 0.703226 and Nd T_{DM} model ages (Tables 4 and 5) more than a billion years older than the age of the rocks. These characteristics are consistent with derivation from hydrous, metasomatized mantle (Peck et al., 2004; Chiarenzelli et al., 2010a) and preclude derivation from typical depleted mantle reservoirs.

The amphibolites and metagabbro samples from across the Lowlands have similar geochemical trends as the Pyrites Complex but vary in detail (Fig. 15). In general, they have flatter and higher REE concentrations than the ultramafic rocks and lack a pronounced Ti anomaly. On the Nd evolution diagram (Fig. 16), they and the Pyrites ultramafic rocks display a relatively steep evolutionary path for mafic and ultramafic rocks, which typically yield poorly constrained model ages because of their low slope (Dickin and McNutt, 2007). However, several anomalies occur. In particular, samples of sheared metagabbroic and phlogopite lamprophyre from the Pyrites Complex have low slopes and yield Nd T_{DM} (1300 Ma) mantle separation ages of 2260 and 2620 Ma, unrealistically older than their possible age range and that of cogenetic samples. Both of these samples have abundant phlogopite, which may have preferentially incorporated Nd.

The Pyrites Complex and Lowlands amphibolite belts form boudins and disrupted belts largely within carbonate rocks of the lower marble. At Pyrites ultramafic rocks are in contact with graphite-bearing, pyritic gneisses interpreted as deep-water, anoxic, and in part, chemogenic muds (Chiarenzelli et al., 2007). They contain a variety of accessory minerals including chromite, sphalerite, pyrrhotite, chalcopyrite, molybdenite, galena, stannite, and V-bearing rutile (Tiedt and Kelson, 2008). The

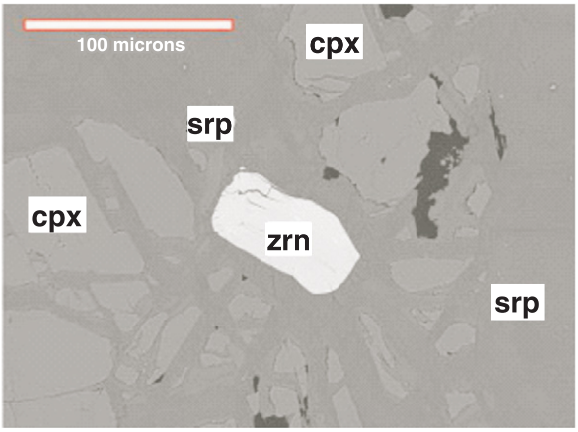

Figure 10. Scanning electron microprobe photomicrograph of a zircon grain in serpentinized pyroxenite (1197 ± 5 Ma) from Pyrites, New York. Cpx—clinopyroxene; srp—serpentine; zrn—zircon. Black areas are the underlying glass slide.

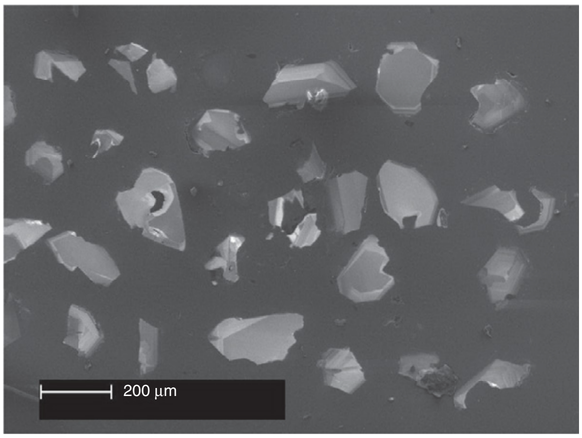

Figure 11. Scanning electron microprobe cathodoluminescence photomicrograph of zircon separated from peridotite (1140 ± 7 Ma, 1202 ± 10 Ma). Note weak zoning in zircons and anhedral to subhedral shapes.

origin of the chromite in the pyritic gneisses may have been, in part, derived from the erosion or slumping of ultramafic rocks along fractures or transform faults or through structural interleaving.

Field investigation reveals that a wide range of metasedimentary lithologies occurs within the pyritic gneisses at Pyrites including pelitic schists and biotite ± garnet ± sillimanite quartzofeldspathic gneisses, pyritic breccias (ore zone), and thin (1–2 cm), fine-grained positively weathering siliceous layers interlayered within garnet-biotite-sillimanite gneisses. Geochemical analyses (Table 8) indicate the pelitic layers in the Popple Hill Gneiss and at Pyrites have compositions similar to that of typical shales, while resistant layers contain up to 80% or more SiO_2. The ore and some pelitic gneisses from Pyrites contain elevated levels of As, Cu, Ni, V, and Zn, among other metals. One sample contained 1.95 wt% MnO. These results suggest the pyritic gneiss sequence includes components of detrital, as well as chemogenic origin, including quartzite units which are interpreted as thin chert layers and metal-rich, hydrothermal, pyritic ore. The occurrence of abundant graphite suggests the depositional environment allowed the preservation of organic matter and was likely reducing. Collectively, the rocks at Pyrites and amphibolitic belts throughout the Lowlands represent a highly dismembered, metamorphosed, and incomplete ophiolitic sequence obducted during Shawinigan orogenesis.

Igneous zircon is an unusual primary phase in ultramafic rocks, and the lack of oscillatory zoning suggests the zircons are of metamorphic origin. Therefore the ages obtained (1140 ± 7 Ma; ca. 1200 Ma–1202 ± 20 and 1197 ± 5) are best interpreted as the timing of metamorphic zircon growth in rocks of the Pyrites Complex. The 1140 ± 7 Ma age postdates intrusion of rocks of the AMCG suite in the Lowlands, but is in good agreement with the U-Pb ages obtained on monazites separated from these rocks (McLelland et al., 1993), presumably cooling to blocking temperatures within tens of millions of years of the AMCG thermal pulse. Carbon and oxygen isotopes from the undeformed calcite veins that hosted some of the zircons recovered from the peridotite sample (1140 ± 7 Ma) plot within the Adirondack retrograde calcite field of Morrison and Valley (1988), suggesting the veins themselves are also post-Shawinigan and AMCG intrusion. The ca. 1200 Ma (1202 ± 20 and 1197 ± 5 Ma) age provides a minimum age for the ultramafic rocks and corresponds to the timing of calc-alkaline intrusion (Antwerp-Rossie suite; ca. 1200 Ma; Wasteneys et al., 1999; Chiarenzelli et al., 2010b) and initiation of Shawinigan dynamothermal events in the Adirondack Lowlands. The probable age of the associated ultramafic-mafic rocks is thought to be ca. 1300, in concert with estimates of the timing of rifting in the Central Metasedimentary Belt (Hanmer et al., 2000; Dickin and McNutt, 2007). The slope of these rocks on a Sm-Nd isochron falls between that of the juvenile crust in the Ontario Central Metasedimentary Belt (1280 Ma; Dickin and McNutt, 2007) and Quebecia (1530 Ma; Dickin and Higgins, 1992) and yields an imprecise age of 1440 ± 170 Ma (Chiarenzelli et al., 2010a).

Other Mafic Suites in the Lowlands

A study of Nd isotopic systematics, geochemistry, and field relations of amphibolites and metagabbros suggests at least three distinct suites of mafic rocks occur in the Lowlands. They include: (1) highly enriched and meta-

TABLE 2. U-Pb SHRIMP ANALYTICAL DATA FROM ZIRCONS SEPARATED FROM PERIDOTITE OF THE PYRITES COMPLEX

Grain spot	U (ppm)	Th (ppm)	Th/U	Pb (ppm)	f206%	$^{207}Pb/^{206}Pb$ 204corr	±1σ (%)	$^{208}Pb/^{206}Pb$ 204corr	±1σ (%)	$^{206}Pb/^{238}U$ 204corr	±1σ (%)	$^{207}Pb/^{235}U$ 204corr	±1σ (%)	%c	$^{206}Pb/^{238}U$ Date (Ma)	$^{207}Pb/^{206}Pb$	±1σ (%)
pp-19.1	365	106	0.29	69	0.059	0.0765	1.00	0.0832	1.75	0.188	1.27	1.985	1.71	100	1112.16	1107	20
pp-3.1	352	83	0.23	67	0.019	0.0769	0.90	0.0695	1.72	0.192	1.27	2.039	1.65	101	1133.56	1119	18
pp-5.1	373	106	0.29	73	0.054	0.077	0.81	0.0828	1.26	0.195	1.27	2.064	1.59	102	1145.86	1120	16
pp-17.1	318	83	0.26	60	0.087	0.0771	0.98	0.0757	1.78	0.191	1.27	2.028	1.7	100	1126.28	1123	20
pp-4.1	328	88	0.27	64	0.01	0.0774	0.86	0.0789	1.39	0.196	1.28	2.094	1.62	102	1154.62	1132	17
pp-21.1	464	154	0.33	90	–0.033	0.0775	0.93	0.0976	1.49	0.192	1.27	2.051	1.66	100	1131.58	1135	19
pp-10.1	405	113	0.28	77	–0.003	0.0776	0.66	0.0815	0.89	0.19	1.27	2.033	1.5	99	1121.37	1137	13
pp-9.1	400	126	0.31	72	0.036	0.0776	0.74	0.086	1.08	0.18	1.27	1.927	1.55	94	1067.05	1138	15
pp-20.1	386	100	0.26	75	0.03	0.0777	0.70	0.0764	1.06	0.197	1.27	2.109	1.53	102	1158.48	1139	14
pp-13.1	538	137	0.25	104	0.023	0.0777	0.86	0.0751	1.72	0.195	1.27	2.087	1.62	101	1146.83	1140	17
pp-18.1	494	152	0.31	95	–0.012	0.0777	0.81	0.0865	1.36	0.191	1.27	2.052	1.59	99	1129.32	1140	16
pp-11.1	466	147	0.32	91	0	0.0778	0.62	0.0954	0.79	0.194	1.27	2.082	1.48	100	1143.29	1142	12
pp-14.1	439	120	0.27	85	0.02	0.0778	0.69	0.0789	1.04	0.195	1.27	2.092	1.52	101	1148.41	1142	14
pp-12.1	567	150	0.27	107	0.036	0.0778	0.60	0.078	0.93	0.19	1.26	2.042	1.47	98	1122.98	1143	12
pp-15.1	326	74	0.23	62	–0.017	0.078	0.78	0.0674	1.28	0.192	1.27	2.064	1.58	99	1131.19	1148	16
pp-22.1	376	96	0.26	74	0.017	0.0781	0.76	0.0763	1.23	0.198	1.27	2.134	1.56	101	1165.27	1150	15
pp-7.1	500	122	0.24	95	–0.032	0.0783	0.82	0.0718	1.67	0.192	1.27	2.078	1.59	98	1134.3	1155	16
pp-1.1	645	191	0.3	126	0.01	0.0786	0.55	0.0887	0.74	0.194	1.26	2.103	1.44	98	1143.66	1161	11
pp-2.1	279	76	0.27	55	–0.024	0.0786	0.88	0.0823	1.35	0.196	1.28	2.122	1.64	99	1153.41	1161	17
pp-6.1	423	113	0.27	84	–0.02	0.0792	0.70	0.0802	1.08	0.199	1.27	2.178	1.52	99	1171.93	1178	14
pp-8.1	295	65	0.22	58	0.007	0.0802	0.75	0.066	1.18	0.199	1.28	2.195	1.56	97	1167.51	1201	15
pp-16.1	388	111	0.29	77	0.003	0.0805	0.68	0.0851	0.92	0.198	1.27	2.192	1.51	96	1162.31	1209	13

Note: f206% = 100 × (common ^{206}Pb/total ^{206}Pb)
$^{207}Pb/^{206}Pb$ 204corr = ^{204}Pb-corrected $^{207}Pb/^{206}Pb$ ratio
$^{206}Pb/^{238}U$ 204corr = ^{204}Pb-corrected $^{206}Pb/^{238}U$ ratio
$^{207}Pb/^{235}U$ 204corr = ^{204}Pb-corrected $^{207}Pb/^{235}U$ ratio
%c = % concordance
$^{207}Pb/^{206}Pb$ date = ^{204}Pb-corrected $^{207}Pb/^{206}Pb$ date. SHRIMP—sensitive high-resolution ion microprobe.

morphosed ultramafic-mafic rocks of the Pyrites Complex, in structural contact with Lowlands supracrustals including pyritic gneisses, with Nd $T_{DM(1300)}$ ages of 1445–1611 Ma and ε_{Nd} of 4.3–5.1 (below that of the depleted mantle curve of De Paolo, 1981); (2) amphibolitic rocks exposed in the Pierrepont amphibolite belt that intrude the Popple Hill Gneiss, have mid-ocean ridge basalt (MORB) to arc tholeiite chemistry, yield shallow Nd evolution pathways that have imprecise Nd model ages (shallow slope), and ε_{Nd} values of 5.4–6.8 that lie on the depleted mantle curve; and (3) amphibolites and metagabbros of calc-alkaline chemistry intrusive into the upper marble near Balmat, with restricted Nd $T_{DM(1210)}$ ages of (1366–1393 Ma), relatively steep Nd evolution curves, and ε_{Nd} of 4.6–4.7 (Fig. 16).

As suggested above, the Pyrites Complex is believed to represent tectonic slivers of the upper mantle, oceanic crust, and overlying sediment that once floored the backarc basin developed between the Adirondack Lowlands and southern Highlands named the Trans-Adirondack backarc basin (Chiarenzelli et al., 2009, 2010b; McLelland et al., 2010). Lamprophyre dikes, which cut the ultramafic rocks, imply intrusion in an extensional tectonic regime. The amphibolitic rocks also have geochemistry characteristics compatible with melting of an enriched mantle wedge (Chiarenzelli et al., 2010a).

The amphibolitic rocks exposed at Pierrepont and intrusive sheets (sills) of amphibolite in the Popple Hill Gneiss are the least enriched in incompatible elements, a hallmark of a depleted mantle source (Figs. 15 and 16); however, they have a positive U and Pb anomaly and a large negative Nb anomaly, perhaps indicating a hybrid source. Likely they represent tapping of melts of asthenosphere centered under the Adirondack backarc during foredeep magmatism or the initial stages of subduction and convergence. Numerous amphibolitic dikes are also known from the Newcomb and Paradox Lake belt in the Adirondack Highlands where they extensively intrude marbles similar to those underlying much of the Lowlands and may be of the same age and origin. Metagabbro and metadiorites with calc-alkaline chemistry from the Balmat area are likely correlative with the Antwerp Rossie suite and related to subduction, closure, and collapse of the Trans-Adirondack backarc basin (Carl, 2000; Chiarenzelli et al., 2010b).

Three samples of amphibolites from the Pierrepont amphibolite belt yield nearly horizontal slopes and a wide range of Nd T_{DM} (1300 Ma) model ages (1160, 1470, and 1730 Ma) and ε_{Nd} values that fall on the depleted mantle evolution curve of De Paolo (1981). Given the low slope

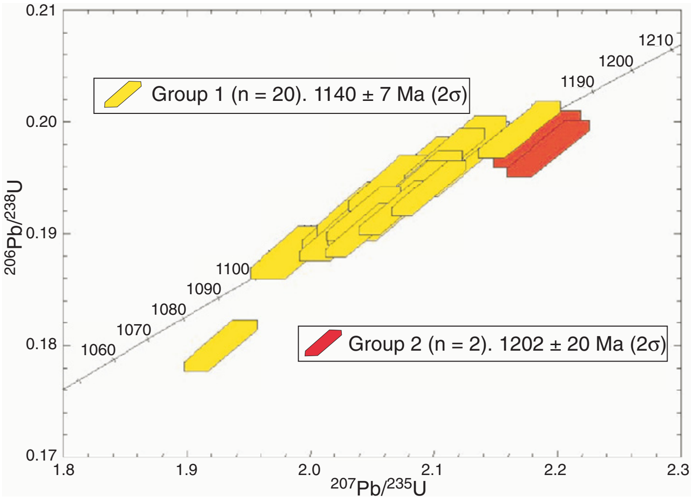

Figure 12. Uranium-lead concordia diagram of zircons separated from an altered peridotite from Pyrites, New York, and analyzed by sensitive high-resolution ion microprobe.

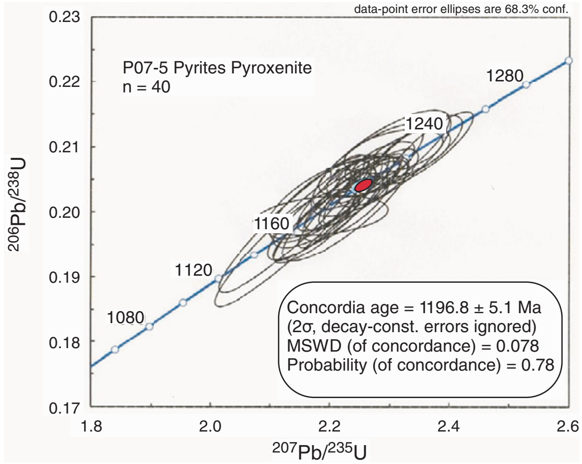

Figure 13. Uranium-lead concordia diagram of zircons separated from a knobby weathering pyroxenite (websterite) from Pyrites, New York, and analyzed by laser ablation–inductively coupled plasma–mass spectrometry. Note that four discordant samples fall off the field of view shown in this concordia diagram. MSWD—mean square of weighted deviates.

of each of the samples, the model ages are likely inaccurate. In particular, the 1160 Ma model age for the cm-scale, layered, clinopyroxene-bearing amphibolite sample from Seven Springs is not geologically reasonable, because it is crosscut by the Hermon granitic gneiss (ca. 1182 Ma). The difference in the slope of the three samples from Pierrepont and those of Pyrites Complex is in agreement with the observations of Tyler (1979), who found substantial variations in major element chemistry between the mafic rocks at Pyrites (Mg rich) and those in the Pierrepont amphibolite belt. The Pierrepont amphibolites are intrusive into the Lowlands supracrustal sequence, particularly garnetiferous pelitic gneisses of the Popple Hill Gneiss, whereas rocks of the Pyrites Complex are in structural contact with the supracrustal rocks and are clearly older than the Pierrepont amphibolites.

Aside from the aforementioned sample from the Pierrepont amphibolite belt with an unrealistically low model age, three samples from the Balmat area have Nd T_{DM} model ages that are very consistent and the youngest amongst the group of samples (1370, 1390, and 1390 Ma) and have similar ε_{Nd} values (4.5–4.7). On the Nd evolution diagram these samples lie along parallel pathways just slightly to the left of the main group containing the Pyrites Complex and bulk of the Lowlands mafic rocks. Because at least one of these samples (Balmat Gabbro) is known to intrude the metasedimentary sequence of the upper marble, they are considered to be mafic equivalents of the Antwerp-Rossie suite (Chiarenzelli et al., 2010b) and likely to be ca. 1210 Ma in age. Therefore, these model ages were calculated at 1210 Ma and indicate that an origin from typical depleted mantle reservoir is unlikely. The Antwerp-Rossie suite displays a wide range of silica concentrations, and recent work (Chiarenzelli et al., 2010b; Regan, 2010) has documented a bimodal composition, with early mafic plutons followed by those of granitic composition.

Figure 15 shows the incompatible element chemistry of each of the ultramafic and mafic suites identified in this paper normalized to primitive mantle values of Sun and McDonough (1989). The range of values from ca. 1160 to 1150 Ma coronitic gabbros of the Adirondack Highlands has been overlain (Regan et al., 2011) for comparison purposes. Coronitic metagabbros in the Adirondacks are spatial and temporally associated with anorthosite massifs and have been considered by some workers as the unfractionated parental magma of the anorthosite massifs. In each case, the older rocks of the Lowlands have many incompatible elements with abundances an order or magnitude greater than those of the coronites. However, aside from enrichment in U and Pb, the mafic rocks from the Pierrepont amphibolite belt have lower concentrations, but similar incompatible element patterns, to the coronites. Samples from Balmat mafic rocks and the Adirondack Lowlands amphibolite belt show incompatible element patterns and Nd evolution pathways similar to the Pyrites Complex suggesting they were derived by partial melting of mantle material of a similar enriched nature.

TOWARD A TECTONIC MODEL FOR THE EVOLUTION OF THE ADIRONDACK LOWLANDS

The Adirondack Lowlands contain an assemblage of rocks that includes metamorphosed siliceous carbonates (in part stromatolitic) and evaporates (upper marble), pelitic, psammitic, and possible volcanoclastic rocks (Popple Hill Gneiss), shallow-water carbonates, metasandstones, and tourmaline-bearing sandstones (lower marble), chemogenic and metalliferous muds, oceanic crust (amphibolites), and ultramafic rocks (mantle). The most likely way to explain this diverse assemblage is tectonic interleaving and the obduction of oceanic crust and upper mantle along the soles of southeast-verging ductile thrusts during Shawinigan orogenesis. The interleaved metasedimentary rocks represent both rift-drift sedimentation (ca. 1300–1250 Ma) and the development and fill of a foreland basin formed during convergence (ca. 1250–1210 Ma). This tectonostratigraphic sequence was intruded by calc-alkaline to transitional mafic to felsic rocks of the Antwerp-Rossie (ca. 1200 Ma), Hermon granitic gneiss (ca. 1182 Ma), Rockport Granite and Hyde School Gneiss suites (ca. 1172 Ma), and members of the AMCG suite (ca. 1155 Ma). The accompanying deformation is largely responsible for the development of the structural grain and major structures observed in the Lowlands. Collectively the lithologies exposed represent the opening and closure of a backarc basin

TABLE 3. U-Th-Pb LA-MC-ICP-MS ANALYTICAL RESULTS FROM ZIRCONS SEPARATED FROM PYRITES COMPLEX PYROXENITE SAMPLES

Analysis	U (ppm)	Th/U	$^{206}Pb/^{204}Pb$	$^{206}Pb^*/^{207}Pb^*$	(±2σ) (%)	$^{207}Pb^*/^{235}U^*$	(±2σ) (%)	$^{206}Pb^*/^{238}U$	(±2σ) (%)	Error corr.	$^{206}Pb^*/^{238}U^*$	(±2σ) (Ma)	$^{207}Pb^*/^{235}U$	(±2σ) (Ma)	%c	$^{207}Pb^*/^{206}Pb^*$	(±2σ) (Ma)
P07-5-29	533	0.27	27062	17.0202	1.7	0.7510	2.0	0.0927	1.0	0.50	571.5	5.5	568.8	8.7	98	558.0	37.8
P07-5-28	979	1.11	27056	13.6925	2.5	1.1476	3.1	0.1140	1.8	0.57	695.7	11.6	776.1	16.8	131	1014.8	51.5
P07-5-26	1184	0.56	23598	13.7958	3.9	1.1618	4.1	0.1162	1.0	0.25	708.9	6.7	782.8	22.1	128	999.6	79.9
P07-5-39	311	1.67	3918	13.6439	2.9	1.5564	4.1	0.1540	2.8	0.70	923.4	24.4	953.0	25.2	107	1022.0	59.4
P07-5-19	788	0.42	36112	13.0159	2.2	1.7789	2.8	0.1679	1.7	0.61	1000.7	15.6	1037.8	18.0	108	1116.7	43.9
P07-5-41	538	0.19	54592	12.9297	1.2	2.0445	2.3	0.1917	1.9	0.84	1130.7	19.9	1130.5	15.6	100	1130.0	24.5
P07-5-34	1031	0.45	47738	12.9208	2.8	1.7264	4.1	0.1618	3.1	0.74	966.6	27.6	1018.4	26.7	111	1131.4	55.6
P07-5-9	104	0.71	10212	12.9065	1.3	2.0843	2.6	0.1951	2.2	0.86	1149.0	23.6	1143.7	17.9	99	1133.6	26.5
P07-5-35	445	0.31	47252	12.7949	1.4	2.1362	3.8	0.1982	3.5	0.93	1165.8	37.6	1160.6	26.2	99	1150.8	27.0
P07-5-24	167	0.45	17492	12.7451	1.9	2.1847	2.7	0.2019	1.9	0.71	1185.7	21.0	1176.2	19.1	99	1158.6	38.5
P07-5-10	277	0.91	29720	12.7068	1.8	2.1932	2.8	0.2021	2.2	0.78	1186.7	23.7	1178.9	19.6	99	1164.5	34.7
P07-5-37	154	0.26	17082	12.6915	1.4	2.1405	4.1	0.1970	3.9	0.94	1159.3	41.1	1162.0	28.4	100	1166.9	27.4
P07-5-1	261	0.91	23786	12.6296	1.4	2.1731	2.1	0.1991	1.5	0.72	1170.2	15.8	1172.5	14.4	100	1176.6	28.5
P07-5-23	216	0.91	23346	12.6132	1.7	2.2632	2.7	0.2070	2.1	0.77	1213.0	23.0	1200.9	19.0	98	1179.2	34.1
P07-5-40	484	0.71	46034	12.6075	1.2	2.2215	2.3	0.2031	1.9	0.85	1192.1	21.0	1187.8	16.0	99	1180.1	23.9
P07-5-2	261	0.83	23780	12.5960	1.4	2.1863	2.7	0.1997	2.3	0.86	1173.8	25.1	1176.7	19.0	100	1181.9	27.7
P07-5-13	791	1.11	55138	12.5861	1.9	2.0355	3.8	0.1858	3.3	0.87	1098.6	33.6	1127.4	26.1	105	1183.4	37.6
P07-5-15	124	0.91	7412	12.5835	3.2	2.1863	3.3	0.1995	1.0	0.30	1172.8	10.7	1176.7	23.2	101	1183.8	62.8
P07-5-4	125	0.67	14184	12.5721	1.9	2.2542	2.2	0.2055	1.0	0.46	1205.0	11.0	1198.1	15.3	99	1185.6	38.2
P07-5-38	410	0.63	46998	12.5641	1.0	2.1745	2.1	0.1981	1.9	0.88	1165.4	19.9	1172.9	14.8	101	1186.9	19.8
P07-5-8	115	0.83	12796	12.5535	1.5	2.2565	1.8	0.2054	1.0	0.55	1204.5	11.0	1198.8	12.7	99	1188.5	29.7
P07-5-14	359	0.67	36668	12.5465	1.0	2.2533	1.5	0.2050	1.2	0.76	1202.4	12.7	1197.8	10.8	99	1189.6	19.8
P07-5-11	238	0.24	25792	12.5322	1.0	2.2040	1.4	0.2003	1.0	0.71	1177.1	10.8	1182.3	9.9	101	1191.9	19.7
P07-5-16	213	1.00	21080	12.5236	2.2	2.2847	3.4	0.2075	2.6	0.76	1215.6	28.6	1207.6	23.9	99	1193.3	43.0
P07-5-17	195	0.67	20590	12.5184	1.3	2.2009	2.8	0.1998	2.5	0.89	1174.4	27.3	1181.3	19.8	101	1194.1	25.2
P07-5-12	870	0.67	63386	12.5180	2.1	2.3060	2.4	0.2094	1.1	0.46	1225.4	12.1	1214.1	16.7	98	1194.1	41.4
P07-5-18	518	0.59	54048	12.5175	1.2	2.2881	1.5	0.2077	1.0	0.65	1216.7	11.1	1208.6	10.9	99	1194.2	23.3
P07-5-33	169	1.00	15866	12.4604	1.0	2.2331	2.6	0.2018	2.4	0.92	1185.0	25.5	1191.5	18.0	101	1203.2	19.7
P07-5-25	927	0.43	89384	12.4530	1.0	2.2339	1.6	0.2018	1.2	0.78	1184.8	13.3	1191.7	11.1	101	1204.4	19.7
P07-5-7	720	0.83	72152	12.4363	1.0	2.2510	1.9	0.2030	1.6	0.84	1191.6	17.2	1197.1	13.1	101	1207.0	19.7
P07-5-5	732	0.37	77868	12.4351	1.4	2.2248	2.1	0.2007	1.6	0.76	1178.8	17.5	1188.9	15.0	102	1207.2	27.4
P07-5-36	428	0.91	48876	12.4243	1.7	2.2252	3.1	0.2005	2.6	0.85	1178.1	28.4	1189.0	21.9	102	1208.9	32.7
P07-5-6	653	0.27	70088	12.4052	1.3	2.2818	1.9	0.2053	1.4	0.75	1203.7	15.7	1206.7	13.5	100	1212.0	25.0
P07-5-30	607	0.83	64542	12.3907	1.0	2.3241	2.1	0.2089	1.9	0.88	1222.7	21.1	1219.7	15.2	100	1214.3	19.7
P07-5-32	148	0.56	16172	12.3612	1.6	2.3312	2.0	0.2090	1.2	0.60	1223.5	13.1	1221.9	14.0	100	1219.0	30.9
P07-5-3	760	0.83	72608	12.3307	1.4	2.3436	2.2	0.2096	1.7	0.77	1226.6	18.5	1225.6	15.4	100	1223.8	27.3
P07-5-31	156	0.63	20014	12.3110	1.0	2.3795	1.4	0.2125	1.0	0.71	1241.9	11.3	1236.5	10.1	99	1227.0	19.7
P07-5-21	343	1.00	43344	12.2592	1.0	2.3857	2.0	0.2121	1.7	0.87	1240.1	19.6	1238.3	14.4	100	1235.2	19.6
P07-5-22B	231	0.53	24574	12.2321	1.0	2.3662	2.0	0.2099	1.7	0.86	1228.4	19.2	1232.5	14.3	101	1239.6	20.2
P07-5-20	531	0.77	63724	12.1924	1.0	2.3779	2.1	0.2103	1.8	0.87	1230.2	20.0	1236.0	14.7	101	1245.9	19.6
P07-5-27	774	1.00	78074	12.0759	1.2	2.4636	2.3	0.2158	2.0	0.86	1259.5	22.3	1261.4	16.4	100	1264.7	22.5

Note: %c = % concordance. *radiogenic Pb. LA-MC-ICP-MS—laser ablation–multicollector–inductively coupled plasma–mass spectrometry.

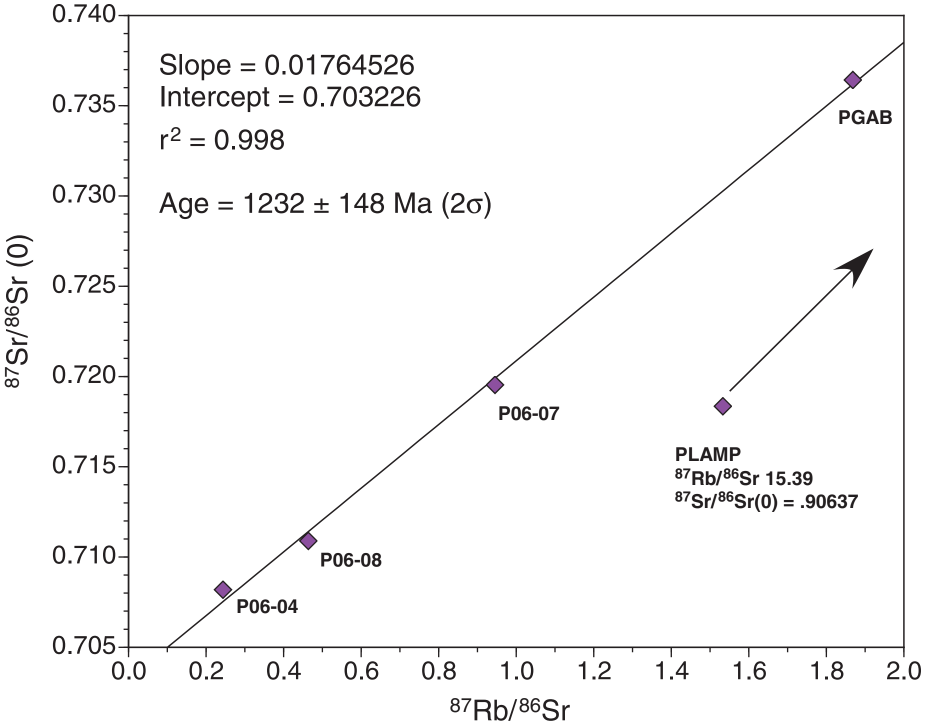

Figure 14. Rubidium-strontium isochron diagram plotting analytical results from rocks of the Pyrites Complex. One sample, that of the lamprophyre dike, plots off the diagram to the upper right (coordinates given).

TABLE 4. RB-SR ISOCHRON DERIVED FROM ROCKS OF THE PYRITES COMPLEX

Sample	Rb (ppm)	Sr (ppm)	$^{87}Sr/^{86}Sr$ (present)	2-sigma	$^{87}Rb/^{86}Sr$	εSr (present)
P06-04 UML	14.5	172.1	0.708188	0.000005	0.2438	52.35
P06-07 GN	54.8	167.9	0.719534	0.000008	0.9455	213.40
P06-08 GN	27.1	169.1	0.710892	0.000009	0.4638	90.73
PGAB GN	76.7	119.1	0.736430	0.000007	1.8686	453.23
PLAMP LP	121.1	23.2	0.906371	0.000007	15.3967	2865.45

Note: GN—gabbronorite; LP—lamprophyre; UML—lherzolite.

that existed between the Frontenac terrane and southern Adirondacks between ~1300 and 1200 million years ago (Fig. 17).

Rift and Drift Stage (ca. 1300–1250 Ma)

Dickin and McNutt (2007) provide Nd isotopic evidence that a backarc rift basin developed underneath most of the Central Metasedimentary Belt at ~1300 million years ago. We propose that a similar, and perhaps synchronous, basin developed between the Frontenac terrane and southern Adirondacks when 1350–1300 Ma tonalitic gneisses of the Dysart–Mount Holly arc rifted away from the margin of Laurentia (McLelland et al., 2010). This basin, named the Trans-Adirondack backarc basin (Chiarenzelli et al., 2009), was floored by oceanic crust, remnants of which are preserved in the Lowlands as disrupted amphibolite belts of the Pyrites Complex. In essence the entire southeast Grenville Province underwent mild extension resulting in a series of isolated rift basins in which much of the area was apparently at or near sea level for extended periods, allowing the accumulation of thick sequences of marbles and quartzites (Hanmer et al., 2000; Dickin and McNutt, 2007).

As no basement rocks have been found, supracrustal rocks in the Lowlands are allochthonous. The oldest U-Pb zircon ages come from calc-alkaline plutonic rocks of the Antwerp-Rossie suite (ca. 1200 Ma). Thin "quartzite" metasandstone units underlie much of the area to the north and west of the Black Lake shear zone in the Frontenac terrane and may well form part of the basal "rift" sequence. However, they are not thick, lack conglomeratic facies, and, in many cases, are more mature than typical rift arkoses. Tourmaline-bearing K-feldspar gneisses are known from the lower marble and may be rift-related, restricted basin arkoses (Brown and Ayuso, 1985). However, this indicates that relatively little of the original rift sequence that led to the development of the Trans-Adirondack Basin is apparently preserved in the Lowlands at the present erosion level. Alternatively, intensive tropical weathering and reworking may have enhanced the maturity of these rocks and/or relatively unique conditions and limited topographic relief occurred during rifting.

Detrital zircons from quartzites (metasandstones) in the Frontenac terrane contain zircons as young as 1301 ± 13 Ma (Sager-Kinsman and Parrish, 1993) and provide a maximum age for their deposition. Here we assume that they either stratigraphically underlie, or are time equivalents of, the lower marble. The lower marble in the Lowlands consists of a wide variety of lithologies including dolomitic marbles, calc-silicate rocks, quartzites, and tourmaline-bearing quartzo-feldspathic gneisses and tourmalinites. Some of these lithologies may be evaporitic in origin and suggest restricted circulation during the initial development of the Trans-Adirondack Basin. As the basin expanded, oceanic crust developed and began to spread, and extensive carbonate deposition occurred on the flanks of the basin. The lower marble was recently dated by Lu-Hf techniques and yielded an age of 1274 ± 9 Ma (Barfod et al., 2005) and is consistent with deposition of the lower marble on the shelf during the drift phase of the Trans-Adirondack Basin.

Basin Fill and Closure (ca. 1250–1210 Ma)

The Elzevirian orogeny (1245–1220 Ma) resulted in deformation and metamorphism associated with the closure of the backarc basin in the Central Metasedimentary Belt (Dickin and McNutt, 2007; Rivers, 2008) and the likely emplacement of the Queensborough ophiolite (Smith and Harris, 1996). In addition, calc-alkaline plutonic rocks of this age are known from the Elzevir terrane and the southern Adirondacks, suggesting much, if not all, of the southern eastern Grenville Province was undergoing compression and subduction at this time. It is therefore likely that the Trans-Adirondack Basin began to collapse during, or shortly after this time.

The Popple Hill Gneiss has yielded detrital zircons as young as 1220 Ma and anatectic zircons from 1180 to 1160 million years in age (Heumann et al., 2006; Bickford et al., 2008) indicating that it was deposited after the Elzevirian orogeny but before Shawinigan orogenesis. In addition, it is cut by plutons of the Antwerp-Rossie suite (ca. 1200 Ma), Hermon granitic gneiss (ca. 1182 Ma), and Hyde School

TABLE 5. SM-ND ISOTOPIC DATA FROM METAMORPHOSED MAFIC AND ULTRAMAFIC ROCKS OF THE ADIRONDACK LOWLANDS AND HIGHLANDS

Sample	Sm (ppm)	Nd (ppm)	$^{147}Sm/^{144}Nd$	$^{143}Nd/^{144}Nd$ (present)	2-sigma	Age (Ma)	εNd (present)	$^{143}Nd/^{144}Nd$ (initial)	CHUR (T_{cry})	εCHUR (T_{cry})	Model age (DM Ma)
Pyrites Complex Adirondack Lowlands; Tc ~1.30–1.35 Ga											
PLAMP LP	9.82	33.73	0.17532	0.512449	0.000004	1300	–3.69	0.510952	0.510959	–0.13	2618
PGAB GN	19.51	66.08	0.17780	0.512578	0.000004	1300	–1.17	0.511060	0.510959	1.98	2258
P06-08 GN	7.34	27.72	0.15945	0.512539	0.000005	1300	–1.93	0.511178	0.510959	4.29	1611
Pyroxenite W	9.27	40.15	0.13904	0.512356	0.000005	1300	–5.50	0.511169	0.510959	4.12	1544
Peridotite UML	14.42	58.69	0.14796	0.512466	0.000003	1300	–3.36	0.511203	0.510959	4.78	1500
P06-07 GN	11.37	51.04	0.13415	0.512345	0.000004	1300	–5.72	0.511200	0.510959	4.72	1472
P06-04 UML	9.23	39.87	0.13941	0.512409	0.000004	1300	–4.47	0.511219	0.510959	5.09	1445
Mafic rocks, Adirondack Lowlands: Tc ~1.30–1.35 Ga											
Bigelow AMP	7.56	30.18	0.15085	0.512443	0.000005	1300	–3.81	0.511155	0.510959	3.84	1624
Antwerp AMP	5.04	16.99	0.17864	0.512742	0.000005	1300	2.03	0.511217	0.510959	5.06	1608
Stellaville AMP	6.45	30.76	0.12627	0.512223	0.000005	1300	–8.10	0.511145	0.510959	3.64	1552
N. Dekalb MG	3.31	14.95	0.13333	0.512297	0.000005	1300	–6.66	0.511158	0.510959	3.91	1548
Potsdam AMP	7.47	37.38	0.12034	0.512190	0.000005	1300	–8.75	0.511162	0.510959	3.98	1508
Pierrepont amphibolites, Adirondack Lowlands; Tc ~1.21 Ga											
Pierrepont AMP	2.17	6.72	0.19446	0.512893	0.000005	1220	4.79	0.511233	0.510959	5.35	1729
Pierrepont AMP	3.90	12.36	0.19001	0.512884	0.000005	1220	4.98	0.511261	0.510959	5.86	1471
7 Springs LA	3.48	10.91	0.19208	0.512948	0.000005	1220	6.04	0.511308	0.510959	6.79	1166
Balmat Antwerp-Rossie suite, Adirondack Lowlands; Tc ~1.21 Ga											
Balmat gabbro MG	28.17	137.68	0.12321	0.512287	0.000005	1200	–6.86	0.511308	0.511075	4.55	1393
Geers Crns. AMP AAMPAMP	7.40	35.69	0.12486	0.512303	0.000005	1200	–6.53	0.511311	0.511075	4.62	1390
S. Balmat MG	9.83	50.76	0.11662	0.512244	0.000005	1200	–7.69	0.511317	0.511075	4.74	1366
Dana Hill metagabbro, Adirondack Highlands; Tc ~1.30–1.35 Ga											
Dana Hill MG	6.27	24.59	0.15355	0.512427	0.000005	1300	–4.11	0.511116	0.510959	3.08	1735

Note: AMP—amphibolite; GN—gabbronorite; LA—layered amphibolite; LP—lamprophyre; MG—metagabbro; UML—lherzolite; W—websterite; CHUR—chondritic uniform reservoir.

TABLE 6. CARBON AND OXYGEN ISOTOPES FROM CALCITE VEINS IN THE PYRITES COMPLEX

Sample	Location	$\delta^{13}C$ (‰, PDB)	$\delta^{18}O$ (‰, PDB)	$\delta^{18}O$ (‰, SMOW)
PY-1	Pyrites	–7.018	–14.775	15.629
PY-2	Pyrites	–6.975	–14.728	15.678
PY-3	Pyrites	–7.358	–14.738	15.668

Note: PDB—PeeDee belemnite; SMOW—standard mean ocean water.

Gneiss (ca. 1172 Ma). These constraints require that it was likely deposited during closing phase of the Trans-Adirondack Basin. If so, it may represent flysch and/or molasse deposition within a foredeep during active tectonism.

After deposition of the lower marble, the Trans-Adirondack Basin began to deepen and accumulate clastic detritus, some turbiditic, and perhaps including a metavolcanic component (Carl, 1988). The production of a linear foredeep is envisioned which was filled by the clastic detritus of the Popple Hill Gneiss, analogous the Ordovician Taconic foredeep of eastern New York and Vermont containing thick sequences of shale, sandstone, and thin ash layers, eventually giving way to the deposition of Silurian evaporates in a restricted basin. Given the time constraints (deposition of the Popple Hill Gneiss after ca. 1220 Ma), the foredeep may well have begun forming during Elzevirian orogenesis (1245–1220 Ma). Because the Popple Hill Gneiss lacks Archean detrital zircons, sediment was likely derived from the southeast and the basin separated from the Superior Province (Bickford et al., 2008). Eventual filling and/or contraction of the basin and restriction from open ocean circulation led to the deposition of the siliceous carbonate-evaporite sequence of the upper marble (deLorraine and Sangster, 1997). Deposition of the upper marble was punctuated by the pulses of sedimentary exhalative massive sulfide (SEDEX) deposition of zinc and lead sulfides derived from metalliferous hydrothermal fluids driven by convergence occurring external to, or beneath, the basin.

Supracrustal rocks of similar age, including highly aluminous metapelites and calc-silicates with minor quartzites and marble, are found in the Shawinigan domain of southwestern Quebec (Martignole, 1978; Corrigan and van Breeman, 1997). A sample of a quartzite layer from the St. Boniface metasedimentary unit contained a variety of detrital zircon populations, the youngest of which yielded a maximum age of 1176 ± 18 Ma. If these supracrustal rocks were deposited within the same backarc basin as supracrustal rocks of the Adirondacks, sedimentation in the northern extension of the basin and its closure outlasted that in the Adirondacks, ~300 km to the S-SE, and attest to asynchronous tectonism across large areas.

Similar supracrustal rocks likely formed on opposing flanks of the basin and record the transition from continued spreading to eventual convergence. Supracrustal rocks similar to those of the metasedimentary sequence in the Adirondack Lowlands are found in Adirondack Highlands. In addition, the Irving Pond quartzite (Peck et al., 2010), with a maximum depositional age of 1300 Ma and overlying 1350–1300 Ma tonalitic gneisses of the southern Adirondacks, may represent coarse clastic deposition, fringing this terrane, which formed during the rift and drifted away from the remainder of Laurentia as the Trans-Adirondack Basin developed. Other rocks such as the Popple Hill Gneiss and upper marble have depositional ages (maximum age of ca. 1220 Ma; Heumann et al., 2006; Bickford et al., 2008) consistent with deposition during or just before Shawinigan contraction, perhaps in restricted basins whose boundaries were imposed by distal structural or tectonic controls of accommodation space.

Subduction, Convergence, and Transitional Magmatism (ca. 1210–1170 Ma)

Mafic dikes and sills, represented by the mafic rocks of the Pierrepont amphibolite belt, of mid-oceanic ridge chemistry and depleted

TABLE 7. WHOLE-ROCK GEOCHEMISTRY OF ROCKS OF THE PYRITES COMPLEX DETERMINED BY XRF (MAJORS) AND ICP-MS (TRACE)

Samples	SV	PY	SS	WP	WP	DH	BL	ND	PD	BG	SB	GC	AN
Lithology	AM	AM	LAM	AM	AM	MG	AM	MG	AM	MG	AM	MG	AM
Latitude (N)	44.4802	44.5215	44.5773	44.5323	44.5323	44.3705	44.4153	44.5117	44.6683	44.2534	44.1783	44.1949	44.1952
Longitude (W)	75.2457	75.1912	74.8635	75.0197	75.0197	75.1617	75.3335	75.3693	74.9891	75.3878	75.3452	75.3452	75.6245
SiO_2	49.05	51.62	46.90	47.66	47.51	47.04	48.20	50.49	47.44	51.15	53.88	48.03	47.47
TiO_2	2.55	1.55	1.53	1.75	0.93	3.63	0.92	0.64	1.56	1.28	1.26	1.35	2.06
Al_2O_3	15.80	18.86	12.94	12.92	14.71	12.69	8.25	15.85	16.87	11.98	17.95	15.04	13.74
Fe_2O_3(T)	13.31	6.78	13.19	15.85	12.58	16.15	12.31	9.40	11.19	10.03	9.05	11.52	15.67
MnO	0.13	0.07	0.23	0.25	0.20	0.21	0.20	0.14	0.17	0.14	0.12	0.14	0.26
MgO	4.58	5.28	6.56	6.95	7.54	4.32	15.27	8.79	6.21	10.24	3.53	6.39	6.11
CaO	7.88	5.41	13.05	10.91	11.53	7.91	10.38	7.74	10.26	7.53	5.77	11.00	9.08
K_2O	1.49	3.20	0.99	0.61	0.60	1.89	0.97	1.99	1.16	2.59	1.84	1.17	0.83
Na_2O	2.82	3.80	2.43	2.09	2.51	3.03	0.90	2.50	3.17	1.82	3.67	3.27	2.41
P_2O_5	0.18	0.69	0.12	0.14	0.08	0.31	0.07	0.09	0.41	0.60	0.36	0.12	0.23
LOI	1.00	2.10	1.90	0.00	1.10	1.20	2.60	1.40	1.30	2.10	1.80	1.00	1.90
Sum	97.96	97.56	98.07	99.23	98.30	97.36	97.60	97.77	98.61	97.62	97.63	98.22	97.99
Ti	15273	9297	9189	10477	5556	21770	5485	3842	9339	7678	7564	8062	12342
P	804	2996	537	616	345	1367	323	402	1769	2616	1559	542	987
Cr	–9	44	211	99	136	–10	391	47	84	391	1	141	103
Ga	22	23	18	19	16	20	12	16	19	18	24	18	19
Ni	1	48	51	38	78	6	158	69	48	140	5	89	56
Rb	35	101	30	8	12	56	39	59	10	69	37	21	19
Sr	650	740	230	121	148	324	56	510	901	438	584	727	167
Cs	1.54	3.65	0.25	0.13	0.15	4.07	2.10	4.76	0.15	3.26	0.58	2.08	0.50
Ba	354	1210	117	51	88	478	71	335	228	502	530	249	160
Sc	23.4	11	47.8	51.6	43.6	28	39.4	24.3	29.1	32.3	16.5	28.1	47.3
V	375	151	335	378	250	336	188	158	233	203	168	265	368
Ta	0.5	0.5	0.3	0.2	<0.2	0.5	0.2	0.3	0.3	0.7	0.5	0.3	0.2
Nb	9	9	4	3	1	7	3	3	6	12	12	5	3
Zr	135	575	87	95	53	210	78	86	150	250	336	67	137
Hf	3.55	13.36	1.87	2.22	1.5	4.82	2.38	2.5	2.6	7.12	6.32	2.84	3.72
Th	3	6	4	5	3	4	11	–1	–16	10	–1	–11	9
U	–2	–2	2	0	3	–1	6	–4	–11	4	–6	–7	3
Pb	3	10	8	6	17	6	9	7	–10	4	1	–2	16
Cu	13	19	52	37	59	15	28	19	61	7	18	22	348
Zn	105	91	111	123	306	132	126	78	110	127	94	187	132
Y	25	24	35	40	26	38	31	21	31	65	37	30	45
La	19	44	–13	–13	12	37	–3	17	14	71	55	2	18
Ce	43	62	19	–7	–5	49	70	35	56	182	107	60	5
Pr	7.31	8.83	2	2.33	1.29	5.19	6.41	3.59	8.4	30.01	12.08	8.11	3.36
Nd	21	37	4	0	7	30	47	13	16	139	58	30	15
Sm	6.45	9.27	3.48	3.9	2.17	6.27	7.56	3.31	7.47	28.17	9.83	7.4	5.04
Eu	1.698	2.236	1.658	1.313	0.777	1.83	1.691	0.866	2.193	5.544	2.637	1.831	1.453
Gd	5.54	7.63	4.38	4.86	2.73	6.74	6.56	3.08	6.68	20.94	8.25	6.62	5.89
Tb	0.79	1.034	0.792	0.894	0.511	1.062	0.957	0.501	0.941	2.657	1.192	0.971	1.045
Dy	4.5	5.3	5.4	5.9	3.5	6.7	5.2	3.1	5.3	12.5	6.7	5.5	6.9
Ho	0.877	0.951	1.17	1.316	0.748	1.369	0.989	0.668	1.046	2.198	1.3	1.07	1.446
Er	2.27	2.34	3.25	3.6	2.09	3.62	2.48	1.85	2.71	5.34	3.33	2.81	4.05
Tm	0.346	0.33	0.5	0.574	0.334	0.544	0.37	0.305	0.41	0.779	0.509	0.428	0.637
Yb	2.147	2.017	3.141	3.747	2.067	3.351	2.302	1.906	2.504	4.884	3.144	2.57	4.029
La/Yb	8.85	21.81			5.81	11.04		8.92	5.59	14.54	17.49	0.78	4.47

Note: Locations: SV—Stellaville; PY—Pyrites; SS—Seven Springs; WP—West Pierrepont; DH—Dana Hill; BL—Bigelow; ND—North DeKalb; PD—Potsdam; BG—Balmat Gabbro; SB—South Balmat; GC—Geers Corners; AN—Antwerp.

Rock type abbreviations: AM—amphibolite; LAM—layered amphibole; MG—metagabbro. ICP-MS—inductively coupled plasma–mass spectrometry; XRF—X-ray fluorescence; LOI—loss on ignition.

mantle Nd signature were injected into the supracrustal sequence as subduction-derived, mafic, calc-alkaline melts were produced during the initial stages of convergence. These were followed closely in time by felsic calc-alkaline melts of the Antwerp-Rossie and later igneous suites with transitional geochemical characteristics including the Hermon, Hyde School–Rockport, and AMCG suites. This magmatism may have been channeled by temporal or spatial variations in deformation as the Antwerp-Rossie suite primarily intrudes the lower marble, the Hermon suite, the Popple Hill Gneiss, and the Hyde School–Rockport suite intrudes across the entire Lowlands-Frontenac region.

A fundamental question in the Adirondack segment of the Grenville orogen is the significance of the Carthage-Colton shear zone. While the late kinematic history of the shear zone is well constrained (Selleck et al., 2005), its early history is less well understood. Kinematic indicators have been used to suggest both strike-slip (Johnson et al., 2004) and reverse motion (Baird, 2006; Wiener et al., 1983). Similarities between supracrustal rocks on both sides of the Carthage-Colton shear zone have led many authors to suggest, or imply, they are part of the same or similar stratigraphic sequence (McLelland and Isashsen, 1986; Wiener, 1983; Heumann et al., 2006; Bickford et al., 2008). Geophysical data (seismic reflection and refraction) have found the upper crust to be homogeneous across the Carthage-Colton shear zone restricting its depth to the upper 2–3 km (Hughes and Luetgert, 1992). These studies confirm that the Carthage-Colton shear zone is not a suture (cf. Mezger et al., 1992), a conclusion also reached by Hanmer et al. (2000) using various lines of geological evidence. We contend that the Carthage-Colton shear zone is the sole of a major Shawinigan ductile fold-and-thrust system reactivated during orogenic collapse (Selleck et al., 2005) and that the differences across it stem primarily from its post-Shawinigan history and erosion level. The incorporation of mantle

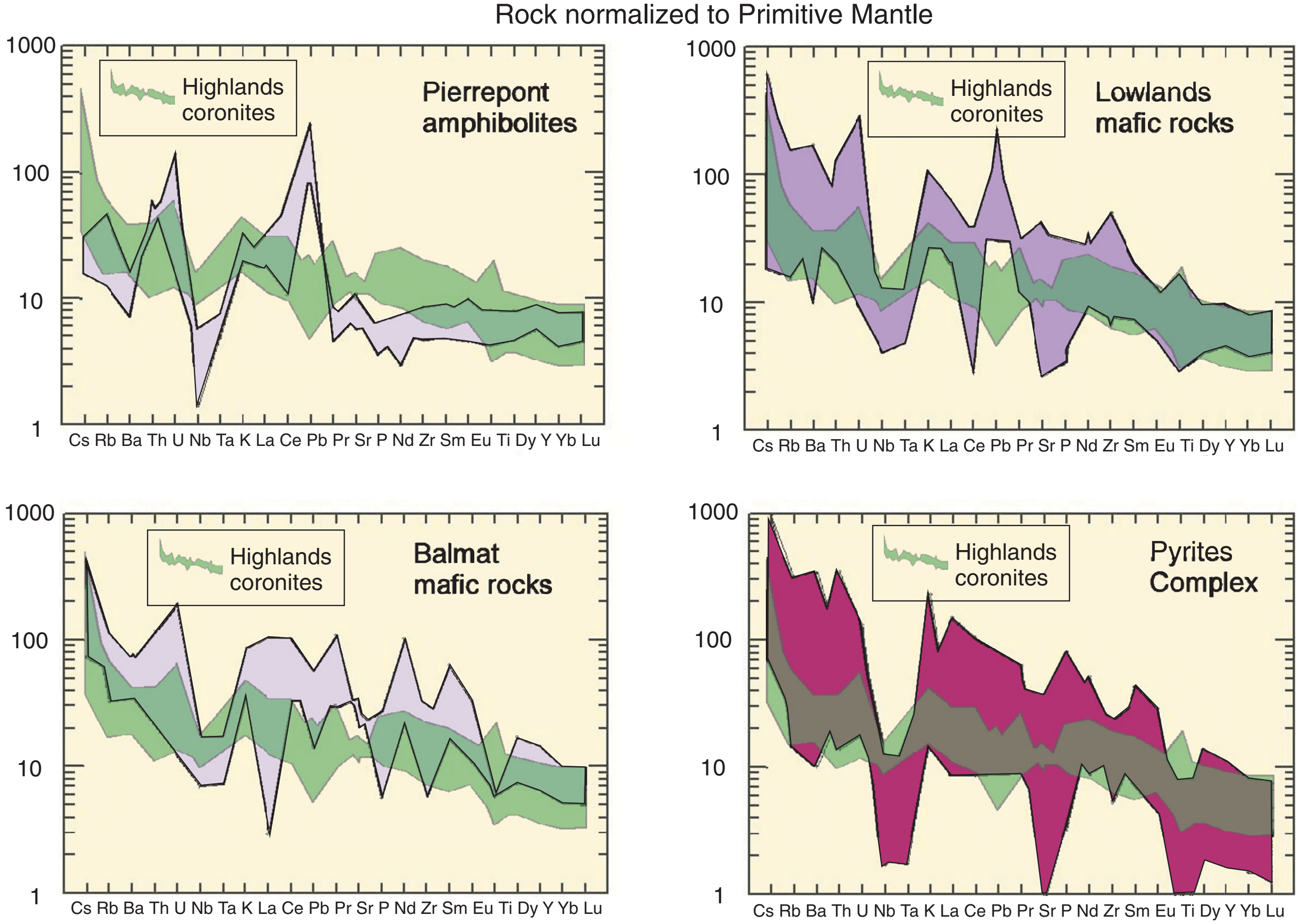

Figure 15. Incompatible element trends of the Pyrites Complex and Adirondack Lowlands mafic rocks normalized to primitive mantle compositions. Overlay shows the composition of Adirondack Highlands coronitic metagabbros from Regan (2010). Coronitic metagabbros are considered the protolith of the anorthosite-mangerite-charnockite-granite massifs and were emplaced after lithospheric delamination following the Shawinigan orogeny. Presumably, they were derived from a previously untapped asthenospheric source.

rocks and oceanic crust in the Adirondack Lowlands metasedimentary sequence requires opening of a basin, the generation of oceanic crust, and temporary separation of the Lowlands and Highlands between ca. 1300–1220 Ma, and eventual redocking of the outboard terranes in the southern Adirondack Highlands resulting in Shawinigan orogenesis. Note that the Dana Hill metagabbro analyzed in this study occurs on the Highlands side of the Carthage Colton mylonite zone and shows similarities to the Pyrites Complex. Other similar ultramafic-mafic bodies have not yet been identified in the Highlands.

Magmatic rocks of the Hermon granitic gneiss (ca. 1182 Ma), Rockport Granite, and Hyde School Gneiss (ca. 1172 Ma) have field relations that indicate intrusion during Shawinigan orogenesis and may have, on a regional scale, led to anatectic melting of the Popple Hill Gneiss (1180–1160 Ma). In addition, their geochemical characteristics are transitional between those of the calc-alkaline Antwerp-Rossie suite and later A-type magmatism of the AMCG suite (1165–1150 Ma) as previously noted by Carl and deLorraine (1997). This suggests that the timing of melts generated by the subduction of oceanic crust of the Trans-Adirondack Basin were followed closely, and/or partially overlapped, by those of the AMCG. Rocks of the AMCG suite have been previously interpreted as the result of lithospheric delamination at end of Shawinigan orogenesis.

CONCLUSIONS

(1) The Pyrites Complex is part of an incomplete, highly deformed and metamorphosed ophiolite obducted during Shawinigan orogenesis between ca. 1200 and 1160 Ma. It contains two populations of small, metamorphic zircons that grew during the initiation of Shawinigan orogenesis (ca. 1200 Ma) and after intrusion of the AMCG suite in the Lowlands and during cooling following its thermal pulse (ca. 1140 Ma).

(2) The Pyrites Complex consists of altered and metamorphosed, upper mantle, ultramafic rocks, oceanic crust (amphibolites and metagabbros), and overlying, and in part chemogenic, metasedimentary rocks (pyritic pelitic gneisses and thin quartzite or chert layers). Evidence of sheeted dikes and pillow lavas is lacking because they were likely obscured during deformation and upper amphibolite facies metamorphism.

(3) The Pyrites Complex originated as part of a backarc basin (Trans-Adirondack backarc basin), which once separated the Frontenac

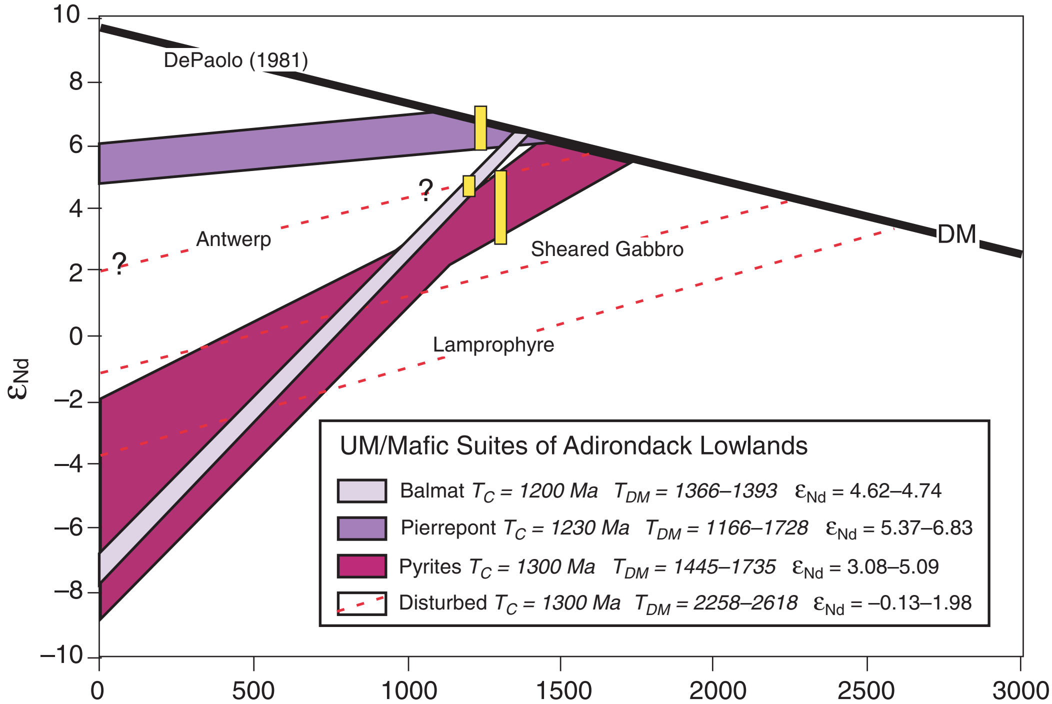

Figure 16. Neodymium evolution diagram for rocks of the Pyrites Complex, Pierrepont amphibolite belt, and Balmat mafic rocks, all exposed in the Adirondack Lowlands.

terrane from the southern Adirondacks and opened synchronously with the backarc basin–failed rift in the Central Metasedimentary Belt delineated by Nd isotopes (Dickin and McNutt, 2007). Broad extension and deposition of carbonate sediments across the Central Metasedimentary Belt at this time is indicated.

(4) The Pyrites Complex is interleaved with metamorphosed sedimentary rocks that formed on the flanks of this basin including the relatively well-preserved metasedimentary sequence in the Adirondack Lowlands. Similar, but less well-preserved metasedimentary rocks, are extensively intruded and disrupted in the Highlands (Chiarenzelli et al., 2011).

(5) Based on available geochronological constraints, the metasedimentary sequence can be subdivided into rocks deposited during the rift-drift (1300–1250 Ma) and basin closure (1250–1210 Ma) phase of the Trans-Adirondack Basin. This was followed by subduction, arc to transitional magmatism, and Shawinigan collisional orogenesis from 1200 to 1160 Ma, ophiolite obduction, and eventual lithospheric delamination and intrusion of the AMCG suite.

(6) The rift sequence, consisting primarily of thin metasandstones (quartzites, maximum age of 1301 Ma), is either poorly preserved, erosionally excised, poorly exposed, or atypical in its lack of coarse clastic and chemically immature, arkosic detritus. Tourmaline-bearing, quartzofeldspathic gneisses are known from the Lowlands, may well be metamorphosed arkosic sandstones, and are candidates for further investigation. The lack of basement rocks in the Lowlands suggests the supracrustal rocks may well be allochthonous. The drift sequence is dominated by thick carbonates of lower marble (ca. 1274 Ma).

(7) The basin closure sequence consists of clastic detritus of the Popple Hill Gneiss (1240–1220 Ma). The Popple Hill Gneiss represents the formation and initial molassoid and flysch fill of a foredeep basin. Filling of the basin and/or continued convergence led to the cessation of clastic deposition and renewed deposition of siliceous marbles and evaporates of the upper marble (ca. 1220–1210 Ma). These rocks, particularly the Popple Hill Gneiss, are extensively intruded mafic sills of MORB to arc tholeiitic chemistry (Carl, 2000). The overall sequence shows many similarities to the Ordovician to Silurian Taconic foreland basin exposed in central New York.

(8) Carbonate deposition of the upper marble was punctuated by the episodic deposition of metalliferous brines resulting in the stratiform sphalerite-pyrite-galena SEDEX deposits. Deposition of the SEDEX horizons was preceded by the deposition of evaporitic rocks. The sequence reflects basin compression, uplift, driving of hydrothermal fluids, and episodic restriction from open ocean circulation. In contrast to the widespread occurrence of rocks likely correlative to the lower marble and Popple Hill Gneiss throughout the Adirondack Region, rocks of the upper marble and associated Pb-Zn deposits are known only in the Lowlands and suggest deposition in a restricted and aerially limited basin or erosional removal.

(9) The Pyrites Complex and metasedimentary rocks of the Adirondack Lowlands are intruded by a wide variety of metaigneous rocks that record the transition from arc to AMCG magmatism. Magmatic rocks of the Antwerp-Rossie suite include early mafic, calc-alkaline tholeiites (ca. 1210 Ma), as well as, slightly younger (ca. 1200 Ma) calc-alkaline tonalites and granites. Subsequent suites including the Hermon granitic gneiss (ca. 1182 Ma), Rockport Granite, and Hyde School Gneiss (ca. 1172 Ma) have transitional geochemical features suggesting the mixing of subduction melts and AMCG magmatism (ca. 1155 Ma), triggered by slab breakoff and lithospheric delamination.

(10) Field relations, geochemistry, and neodymium isotopes can be used to distinguish three suites of mafic rocks in the Lowlands including the Pyrites Complex, MORB-like basalts of the Pierrepont amphibolite belt, and

TABLE 8. GEOCHEMISTRY OF PYRITIC GNEISSES AND ORE FROM THE PYRITES AND SAMPLES OF THE POPPLE HILL GNEISS COMPARED TO UCC VALUES OF RUDNICK AND GAO (2003)

Elements		PH1	PH2	P-S	P-2	P-7	P-8	P-9	Pyrites	UCC*
Lithology	Samples	PG	PG	PG	PG	QT	PG	PG	Ore	R&G
SiO_2	(%)	66.72	67.11	62.45	60.6	80.46	56.48	52.81	36	66.6
TiO_2	(%)	0.4	0.41	0.99	0.68	0.23	0.81	0.77	0.39	0.64
Al_2O_3	(%)	15.42	15.7	20.65	16.86	6.27	18.04	12.56	6.76	15.4
Fe_2O_3	(%)	3.48	3.4	2.51	9.00	4.6	9.62	16.55	33.74	5.04
MnO	(%)	0.1	0.09	0.01	0.04	0.07	1.95	0.79	0.02	0.1
MgO	(%)	1.25	1.2	0.8	1.4	2.69	4.59	6.04	1.52	2.48
CaO	(%)	3.53	3.71	0.08	0.38	0.51	1.5	0.52	0.22	3.59
K_2O	(%)	3.78	3.62	7.09	4.19	1.84	2.27	1.15	2.91	2.80
Na_2O	(%)	3.34	3.42	0.29	0.47	0.51	0.35	0.03	0.16	3.27
P_2O_5	(%)	0.16	0.2	<0.01	0.12	0.02	0.24	0.17	0.23	0.15
Cr_2O_3	(%)	<0.002	<0.002	0.007	0.009	0.007	0.007	0.013	0.015	0.015
TOT/S	(%)	<0.02	<0.02	0.58	4.57	1.54	1.83	3.37	22.78	0.006
LOI	(%)	1.6	0.9	4.8	6	2.7	3.8	8.4	17.8	
Sum	(%)	99.75	99.75	99.73	99.78	99.9	99.63	99.78	99.82	
Ga	(ppm)	19	18.1	24	16.2	8.5	22	18.8	6.4	17.5
Ni	(ppm)	<20	<20	28	83	66	40	117	104	47
Rb	(ppm)	129.6	124	147.4	113.6	41.8	73.9	53	40.9	84
Sr	(ppm)	723.3	783	189	65	26.5	56.9	41.6	32.5	320
Cs	(ppm)	4.9	4.6	6.4	3.7	3.1	4	6.3	0.9	4.9
Ba	(ppm)	1055	1019	1098	775	355	681	346	384	628
Sc	(ppm)	6	6	16	9	7	16	16	5	14
V	(ppm)	56	54	169	304	113	180	208	273	97
Ta	(ppm)	1.4	1.6	1.4	1.1	0.3	0.5	0.5	0.4	0.9
Nb	(ppm)	20.9	23	17.5	15	4.1	10.3	7.6	5.8	12
Zr	(ppm)	134.7	156.5	315.9	166.5	78	401.1	176.4	78.8	193
Hf	(ppm)	3.5	5.6	10.6	5.4	2.2	12.5	5.1	2.2	5.3
Th	(ppm)	8.4	7.9	15	10.6	3.1	13.2	5.6	4.6	10.5
U	(ppm)	4.5	3.1	4.5	4.5	1.3	5.3	2.2	2	2.7
Pb	(ppm)	1.9	2.2	5.7	4.5	11.2	8	19.1	17.3	17
Cu	(ppm)	2.5	2.1	2.7	19.4	46.3	39.1	35	348.3	28
Zn	(ppm)	41	39	17	37	77	583	93	25	67
Co	(ppm)	5.1	4.8	6.4	13.4	17	6.9	20.6	54.8	17.3
Mo	(ppm)	0.3	0.3	1.3	9.1	1.3	2.9	3.7	13.4	1.1
Y	(ppm)	16	17.4	63.5	41.3	16.8	85.5	36.4	15.7	21
La	(ppm)	26.9	32.7	70.3	36.5	14.7	50.1	20.5	9.1	31
Ce	(ppm)	54.1	65	162.8	71.2	29.3	96.9	42	15.7	63
Pr	(ppm)	6.4	7.43	20.64	9.44	4.09	13.91	6.09	1.9	7.1
Nd	(ppm)	25.2	31.1	90.2	40	17.6	58.4	26.1	7.9	27
Sm	(ppm)	3.63	4.04	14.91	6.88	3.03	10.99	5.8	1.8	4.7
Eu	(ppm)	1.04	1.14	3.24	1.2	0.65	2.07	1.15	0.57	1.0
Gd	(ppm)	2.95	3.17	12.57	6.33	2.85	12.32	5.97	1.57	4.0
Tb	(ppm)	0.49	0.52	2.08	1.1	0.48	2.29	0.98	0.32	0.7
Dy	(ppm)	2.81	2.81	11.79	6.56	2.58	13.28	5.84	2.0	3.9
Ho	(ppm)	0.51	0.51	2.19	1.31	0.56	2.9	1.13	0.42	0.83
Er	(ppm)	1.6	1.56	6.2	3.73	1.71	8.07	3.25	1.57	2.3
Tm	(ppm)	0.27	0.27	0.94	0.63	0.32	1.21	0.54	0.21	0.3
Yb	(ppm)	1.72	1.83	5.64	3.77	2.08	7.05	3.25	1.24	1.96
Lu	(ppm)	0.3	0.31	0.87	0.57	0.36	1.08	0.49	0.22	0.31

Note: Location key: PH—samples from the Popple Hill Gneiss; P—samples from Pyrites. Lithology key: PG—pelitic gneiss; QT—aluminous quartzite; Ore—pyritic breccias; UCC—upper continental crust from Rudnick and Gao (2003).

mafic members of the Antwerp-Rossie suite, including coarse-grained gabbros and diorites. They represent different stages in the tectonic history of the Trans-Adirondack Basin.

SUMMARY

While many questions and details remain, taken together these observations suggest that this portion of the SE margin of Laurentia evolved from a rifted margin to a backarc basin to a subduction complex, and accretionary orogen between ca. 1300 and 1160 Ma. The rifted margin was located along, or near the Black Lake shear zone, the boundary between the Frontenac terrane and Adirondack Lowlands (Peck et al., 2004; Chiarenzelli et al., 2010b). The Trans-Adirondack backarc basin formed ca. 1300 Ma as tonalitic arc rocks of the southern Adirondacks rifted away from Laurentia. Sedimentary rocks, including quartzites and marbles were deposited along both flanks of the Trans-Adirondack Basin during drift. Initial docking of the Composite Arc Belt occurred during the earlier Elzevirian orogeny (ca. 1245–1220 Ma) to the NW and deformation and subduction stepped outward into the Trans-Adirondack Basin. Eventually, NW-directed subduction and convergence led to collision of the southern Adirondacks and the Dysart–Mount Holly complex (Adirondis of Gower, 1996) with the Laurentian margin between 1200 and 1160 Ma. Sedimentation, dominated by carbonate deposition during the drift phase (lower marble), gave way to the development of a foredeep basin whose molassoid fill was dominated by clastic detritus of the Popple Hill Gneiss whose detrital zircons suggest a maximum depositional age of ca. 1220 Ma. With further convergence and episodic restricted circulation from the open ocean, siliceous carbonates, evaporates, and SEDEX deposits of the upper marble were deposited in the collapsing basin. The entire sequence was deformed and intruded by calc-alkaline to transitional magmas of the Antwerp-Rossie (ca. 1210–1200 Ma), the Hermon granitic gneiss (ca. 1182), the Rockport Granite, and Hyde School Gneiss (ca. 1172), and eventually by late synorogenic to postorogenic AMCG plutons (ca. 1155 Ma). The Pyrites Complex is an example of the oceanic crust and upper mantle of the Trans-Adirondack Basin and was obducted and interleaved with the supracrustal rocks of the Lowlands during Shawinigan orogenesis.

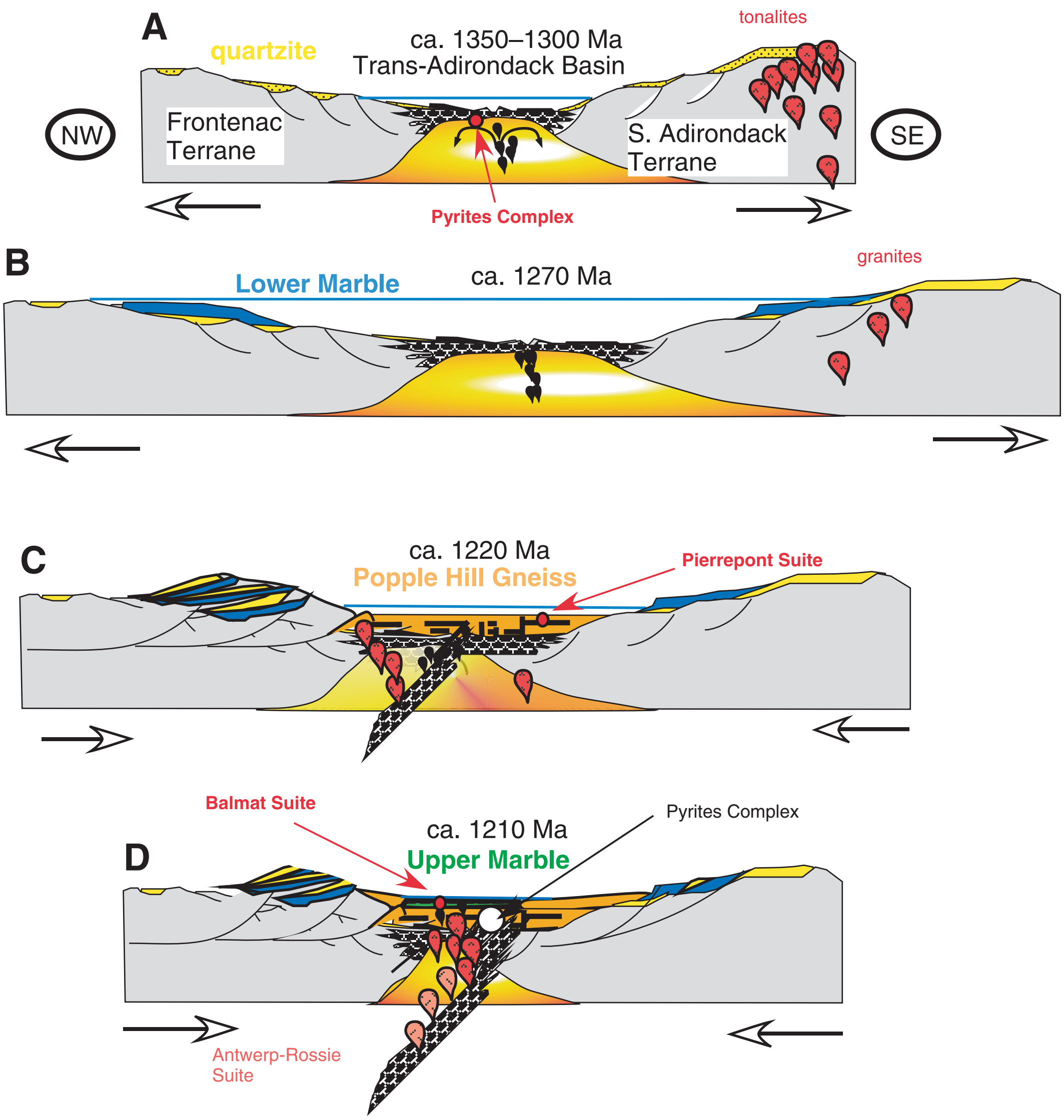

Figure 17. Tectonostratigraphic evolution of the Trans-Adirondack Basin leading up to, and during the initial stages of, Shawinigan orogenesis. Not to scale and with vertical exaggeration. (A) Between 1350 and 1300 Ma and perhaps synchronous with subduction and tonalitic arc magmatism (McLelland and Chiarenzelli, 1990), the southern Adirondacks began rifting away from the Laurentian margin. The 1350–1300 Ma tonalites there are crosscut by amphibolite dikes—perhaps an early manifestation of this rifting event. Within the basin (Trans-Adirondack Basin), mafic volcanism begins to build oceanic crust (Pyrites Complex and Lowlands amphibolite belts), and subsidence results in eventual flooding by sea water (Chiarenzelli et al., 2010a). Sedimentary rocks deposited include metasandstones (quartzites), limey sands (calc-silicate gneisses), tourmalinites, and chemogenic sediments deposited in the flanks and depths of the developing backarc basin. (B) At ca. 1270 Ma (Barfod et al., 2005), the basin continues to expand and is filled with sea water. The quartzites, marbles, calc-silicates, and other facies of lower marble are deposited in shallow, clear water. In response to continued subduction to the NW (subduction zone off diagram to SE), calc-alkaline plutonism continues in the southern Adirondacks where 1250 Ma plutonic rocks have been identified. The production of mafic melts was continuous along the nascent mid-ocean ridge in the Trans-Adirondack Basin. (C) By 1220 Ma, the basin is under compressional stress, likely associated with Elzevirian orogenesis (1245–1225 Ma). Loading of the crust by SE-directed thrusting of the Frontenac terrane converts the Trans-Adirondack Basin into a foreland basin resulting in deepening of the basin and deposition of pelitic and pssamitic gneisses of the Popple Hill Gneiss. Continuing subduction toward the NW may have led to the fallout of volcanic components into the basin (Carl, 1998). Loading and flexure of the crust leads to periodic tapping of mafic magmas injected as sills and dikes into the Popple Hill Gneiss and lower marble in the Lowlands (Pierrepont suite) and equivalent units in the Highlands. Some of these may have extruded onto the seafloor's surface at Seven Springs. (D) Continued compression leading up to the Shawinigan orogeny results in eventual shrinking, filling, and uplift of the basin, resulting in shallow-water, carbonate-evaporite depositional sequence of the upper marble (deLorraine and Sangster, 1997). Intermittent pulses of contraction lead to the migration and outbreak of basinal brines depositing the Zn-Pb sedimentary exhalative massive sulfide deposits of the upper marble, which overly evaporate deposits. Continued subduction, immediately preceding closure and widespread deformation of the Trans-Adirondack Basin, results in intrusion of the Antwerp-Rossie suite at 1210–1200 Ma (Wasteneys et al., 1999; Chiarenzelli et al., 2010b). Of calc-alkaline character, the Antwerp-Rossie suite is bimodal with a minor component of mafic material such as the Balmat suite, which intrudes the upper marble sequence (Carl, 2000). The Black Lake shear zone develops at or near the Laurentian margin, and calc-alkaline magmatism of the Antwerp-Rossie suite is focused east of the shear zone. Eventually the subducting slab detaches, allowing delamination of the lithosphere, and transitional melts of the Hermon granitic gneiss and Hyde School Gneiss suites (ca. 1182–1172 Ma). Eventually after final docking of the Adirondacks to the Frontenac terrane, anorthosite-mangerite-charnockite-granite plutons intrude across the entire area (ca. 1165–1155 Ma).

ACKNOWLEDGMENTS

The authors would like to acknowledge funding from St. Lawrence University and the New York State Museum to carry out the analyses presented in this manuscript. The authors are indebted to the critical review efforts of Drs. Toby Rivers and Michael Hudson, and one unidentified reviewer. We would like to thank our colleagues Drs. Jim McLelland, Bruce Selleck, and David Valentino for many stimulating discussions on Adirondack geology. National Science Foundation grant EAR-0732436 is acknowledged for support of the Arizona LaserChron Center. The editorial staff of *Geosphere*, particularly Dr. Carol Frost, is thanked for their time and effort.

REFERENCES CITED

Baird, G.B., 2006, The strain and geometry of meso-scale ductile shear zones and the associated fluid flow [Ph.D. thesis]: Twin Cities, University of Minnesota, 180 p.

Barfod, G.H., Krogstad, E.J., Frei, R., and Albarède, F., 2005, Lu-Hf and PbSL geochronology of apatites from Proterozoic terranes: A first look at Lu-Hf isotopic closure in metamorphic apatite: Geochimica et Cosmochimica Acta, v. 69, p. 1847–1859, doi: 10.1016/j.gca.2004.09.014.

Bickford, M.E., McLelland, J.M., Selleck, B.W., Hill, B.M., and Heumann, M.J., 2008, Timing of anatexis in the eastern Adirondack Highlands: Implications for tectonic evolution during ca. 1050 Ma Ottawan orogenesis: Geological Society of America Bulletin, v. 120, p. 950–961, doi: 10.1130/B26309.1.

Brown, C.E., 1988, Geology of the Birch Creek area, St. Lawrence County, New York: U.S. Geological Survey Miscellaneous Investigation Series, Map I-1645, scale 1:12,000.

Brown, C.E., 1989, Geologic map of the Beaver Creek area in the Grenville Lowlands, St. Lawrence County, New York: U.S. Geological Survey Miscellaneous Investigation Series Map I-1725.

Brown, C.E., and Ayuso, R.A., 1985, Significance of tourmaline-rich rocks in the Grenville Complex of St. Lawrence County, New York: U.S. Geological Survey Bulletin 1626-C, p. 1–33.

Brown, J.S., 1932, Natural gas, salt, and gypsum in Precambrian rocks at Edwards, New York: American Association of Petroleum Geologists Bulletin, v. 16, no. 8, p. 727–735.

Buddington, A.F., 1939, Adirondack igneous rocks and their metamorphism: Geological Society of America Memoir 7, 354 p.

Carl, J.D., 1988, Popple Hill Gneiss as dacite volcanic: A geochemical study of mesosome and leucosome, northwest Adirondacks, New York: Geological Society of America Bulletin, v. 100, p. 841–849, doi: 10.1130/0016-7606(1988)100<0841:PHGADV>2.3.CO;2.

Carl, J.D., 2000, A geochemical study of amphibolite layers and other mafic rocks in the NW Adirondack Lowlands, New York: Northeastern Geology and Environmental Sciences, v. 22, p. 142–166.

Carl, J.D., and deLorraine, W., 1997, Geochemical and field characteristics of the metamorphosed granitic rocks, NW Adirondack Lowlands, New York: Northeastern Geology and Environmental Sciences, v. 19, p. 276–301.

Carr, S.D., Easton, R.M., Jamieson, R.A., and Culshaw, N.G., 2000, Geologic transect across the Grenville orogen of Ontario and New York: Canadian Journal of Earth Sciences, v. 37, p. 193–216, doi: 10.1139/cjes-37-2-3-193.

Chiarenzelli, J., Lupulescu, M., Cousens, B., Thern, E., and Nelson, D., 2007, Recognition of oceanic crust in the Adirondack Lowlands: Geological Society of America Abstracts with Programs, v. 39, p. 335.

Chiarenzelli, J., Regan, S., and LaVack, C., 2009, The Trans-Adirondack Basin: Precursor to the Shawinigan orogeny: Geological Society of America Abstracts with Programs, v. 41, p. 435.

Chiarenzelli, J., Lupulescu, M., Cousens, B., Thern, E., Coffin, L., and Regan, S., 2010a, Enriched Grenvillian lithospheric mantle as a consequence of long-lived subduction beneath Laurentia: Geology, v. 38, p. 151–154, doi: 10.1130/G30342.1.

Chiarenzelli J., Regan, S., Peck, W., Selleck, B., Baird, G. and Shrady, C., 2010b, Shawinigan magmatism in the Adirondack Lowlands as a consequence of closure of the Trans-Adirondack backarc basin: Geosphere, v. 6, p. 900-916, doi:10.1130/GES00576.1.

Chiarenzelli, J., Valentino, D. W., Lupulescu, M., Thern, E. and Johnston, S., 2011, Differentiating Shawinigan and Ottawan orogenesis in the central Adirondacks: Geosphere, v. 7, p. 2-22, doi:10.1130/GES00583.1.

Coffin, L.M., 2008, A petrographic and geochemical study of mafic and ultramafic rocks from the Grenville Supergroup, Adirondack Lowlands area, New York [B.S. thesis]: Ottawa, Canada, Carleton University, 56 p.

Corrigan, D., and van Breeman, O., 1997, U-Pb age constraints for the lithotectonic evolution of the Grenville Province along the Mauricie transect, Quebec: Canadian Journal of Earth Sciences, v. 34, p. 299–316, doi: 10.1139/e17-027.

Cousens, B.L., 1996, Magmatic evolution of Quaternary mafic magmas at Long Valley caldera and the Devils Postpile, California: Effects of crustal contamination on lithospheric mantle-derived magmas: Journal of Geophysical Research, v. 101, p. 27673–27689.

Cousens, B.L., Aspler, L.B., Chiarenzelli, J.R., Donaldson, J.A., Sandeman, H., Peterson, T.D., and LeCheminant, A.N., 2001, Enriched Archean lithospheric mantle beneath western Churchill Province tapped during Paleoproterozoic orogenesis: Geology, v. 29, p. 827–830, doi: 10.1130/0091-7613(2001)029<0827:EALMBW>2.0.CO;2.

Cousens, B.L., Prytulak, J., Henry, C.D., Alcazar, A., and Brownrigg, T., 2008, The geology, geochronology and geochemistry of the Miocene–Pliocene Ancestral Cascades arc, northern Sierra Nevada, California and Nevada: The roles of the upper mantle, subducting slab, and the Sierra Nevada lithosphere: Geosphere, v. 4, p. 829–853, doi: 10.1130/GES00166.1.

Dahl, P., Hudson, M., Foland, K., Loehn, C., Liogys, V., and Tracy, R., 2005, Evidence of Ottawan overprinting in the Adirondack Lowlands, with implications for Lowland-Highland juxtaposition history: Geological Society of America Abstracts with Programs, v. 37, p. 8.

deLorraine, W.F., and Sangster, A.L., 1997, Geology of the Balmat Mine, New York: Field Trip A5, Geological Association of Canada and Mineralogical Association of Canada Joint Annual Meeting, Ottawa, 43 p.

De Paolo, D.J., 1981, Neodymium isotopes in the Colorado Front Range and crust-mantle evolution in the Proterozoic: Nature, v. 291, p. 193–197, doi: 10.1038/291193a0.

Dickin, A.P., and Higgins, M.D., 1992, Sm/Nd evidence for a major 1.5 Ga crust-forming event in the central Grenville Province: Geology, v. 20, p. 137–140, doi: 10.1130/0091-7613(1992)020<0137:SNEFAM>2.3.CO;2.

Dickin, A.P., and McNutt, R.H., 2007, The Central Metasedimentary Belt (Grenville Province) as a failed backarc rift zone: Nd isotope evidence: Earth and Planetary Science Letters, v. 259, p. 97–106, doi: 10.1016/j.epsl.2007.04.031.

Easton, R.M., 1992, The Grenville Province and the Proterozoic history of central and southern Ontario, *in* Thurston, P.C., ed., Geology of Ontario: Ontario Geological Survey, Special Volume 4, Part 2, p. 714–904.

Gower, C.F., 1996. The evolution of the Grenville Province in eastern Labrador, Canada, *in* Brewer, T.S., ed., Precambrian Crustal Evolution in the North Atlantic Region: The Geological Society of London Special Publication 112, p. 197–218.

Hanmer, S., Corrigan, D., Pehrsson, S., and Nadeau, L., 2000, SW Grenville Province, Canada: The case against post–1.4 Ga accretionary tectonics: Tectonophysics, v. 319, p. 33–51, doi: 10.1016/S0040-1951(99)00317-0.

Heumann, M.J., Bickford, M.E., Hill, B.M., McLelland, J.M., Selleck, B.W., and Jercinovic, M.J., 2006, Timing of anatexis in metapelites from the Adirondack lowlands and southern highlands: A manifestation of the Shawinigan orogeny and subsequent anorthosite-mangerite-charnockite-granite magmatism: Geological Society of America Bulletin, v. 118, p. 1283–1298, doi: 10.1130/B25927.1.

Hudson, M.R., and Dahl, P.S., 1998, The origin of garnetiferous mylonitic gneisses in chill margins of the Hyde School Gneiss, NE Adirondacks, New York: Geological Society of America Abstracts with Programs, v. 30, p. A280–A281.

Hudson, M.R., Dahl, P.S., Loehn, C.W. III, Tracy, R.J., Liogys, V.A., Dria, H., and Petruzzi, N., 2004, Monazites in the NW Adirondack Lowlands record evidence of the Ottawan orogeny: Geological Society of America Abstracts with Programs, v. 36, no. 5, p. 135.

Hudson, M.R., Loehn, C.W., Dahl, P.S., and Kozak, A.L., 2008, Mesoproterozoic Thermotectonic History of the Adirondack Lowlands, New York: Evidence from Monazite Geochronology: Geological Society of America Abstracts with Programs, v. 40, p. 236.

Hughes, S., and Luetgert, J.H., 1992, Crustal structure of the southeastern Grenville Province, northern New York State and eastern Ontario: Journal of Geophysical Research, v. 97, p. 17,455–17,479, doi: 10.1029/92JB01793.

Johnson, E.L., Goergen, E.T., and Fruchey, B.L., 2004, Right lateral oblique slip movements followed by post-Ottawan (1050–1020 Ma) orogenic collapse along the Carthage-Colton shear zone: Data from the Dana Hill metagabbro body, Adirondack Mountains, New York: Geological Society of America, v. 197, p. 357–378, doi: 10.1130/0-8137-1197-5.357.

Lupulescu, M., Chiarenzelli, J., Cousens, B., Thern, E., and Nelson, D., 2008, Mineralogy and geochemistry of a mafic-ultramafic intrusion from Pyrites, Adirondack Lowlands, New York: Geological Society of America Abstracts with Programs, v. 43, p. 80.

Marcantonio, F., McNutt, R.H., Dickin, A.P., and Heaman, L.M., 1990, Isotopic evidence for the crustal evolution of the Frontenac arch in the Grenville Province of Ontario, Canada: Chemical Geology, v. 83, p. 297–314, doi: 10.1016/0009-2541(90)90286-G.

Martignole, J., 1978, Le Précambrien dans le sud de la province teconique de Grenville (Bouclier Canadien). Mémoire depose à l'Université de Montréal, Montréal, Quebec.

McLelland, J., Selleck, B., and Bickford, M.E., 2010, Review of the Proterozoic evolution of the Grenville Province, its Adirondack outlier, and the Mesoproterozoic inliers of the Appalachians, *in* Tollo, R.P., Bartholomew, M.J., Hibbard, J.P., and Karabinos, P.M., eds., From Rodinia to Pangea: The Lithotectonic Record of the Appalachian Region: Geological Society of America Memoir 206, p. 21-49, doi:10.1130/2010.1206(02).

McLelland, J.M., and Chiarenzelli, J.R., 1990. Geochronological studies of the Adirondack Mountains, and the implications of a Middle Proterozoic tonalite suite, *in* Gower, C., Rivers, T., and Ryan, C., eds., Mid-Proterozoic Laurentia-Baltica: Geological Association of Canada Special Paper 38, p. 175–194.

McLelland, J.M., and Isachsen, Y.W., 1986, Geological synthesis of the Adirondack Mountains and their tectonic setting in the SW Grenville Province, *in* Moore, J., Davidson, A. and Baer, A.J., eds., The Grenville Province: Geological Association Canada Special Paper 31, p. 327–339.

McLelland, J.M., Chiarenzelli, J., and Perham, A., 1992, Age, field, and petrological relationships of the Hyde School gneiss, Adirondack lowlands, New York: Criteria for an intrusive origin: The Journal of Geology, v. 100, p. 69–90, doi: 10.1086/629572.

McLelland, J.M., Daly, J.S., and Chiarenzelli, J.R., 1993, Sm-Nd and U-Pb isotopic evidence of juvenile crust in the Adirondack Lowlands, and implications for the evolution of the Adirondack Mountains: The Journal of Geology, v. 101, p. 97–105, doi: 10.1086/648198.

McLelland, J.M., Daly, S.J., and McLelland, J.M., 1996, The Grenville orogenic cycle (ca. 1350–1000 Ma): An Adirondack perspective: Tectonophysics, v. 265, p. 1–28, doi: 10.1016/S0040-1951(96)00144-8.

Mezger, K., Rawnsley, C.M., Bohlen, S.R., and Hanson, G.N., 1991, U-Pb garnet, sphene, monazite, and rutile ages: Implications for the duration and cooling histories, Adirondack Mountains, New York: The Journal of Geology, v. 99, p. 415–428, doi: 10.1086/629503.

Mezger, K., van der Pluijm, B.A., Essene, E.J., and Halliday, A.N., 1992, The Carthage-Colton mylonite zone

(Adirondack Mountains, New York): The site of a cryptic suture in the Grenville orogen?: The Journal of Geology, v. 100, p. 630–638, doi: 10.1086/629613.

Morrison, J., and Valley, J.M., 1988, Post-granulite facies fluid infiltration in the Adirondack Mountains: Geology, v. 16, p. 513–516, doi: 10.1130/0091-7613(1988)016<0513:PGFFII>2.3.CO;2.

Nelson, D.R., 1997, Compilation of SHRIMP U-Pb zircon geochronology data, 1996: Geological Survey of Western Australia, Record 1997/2, 189 p., doi: 10.1016/S0040-1951(96)00144-8

Peck, W.H., Valley, J.W., Corriveau, L., Davidson, A., McLelland, J., and Farber, D.A., 2004, Oxygen-isotope constraints on terrane boundaries and origin of 1.18–1.13Ga granitoids in the southern Grenville Province, *in* Tollo R.P., Corriveau L., McLelland J., and Bartholomew M.J., eds., Proterozoic Tectonic Evolution of the Grenville Orogen in North America: Boulder, Colorado, Geological Society of America Memoir 197, p. 163–182.

Peck, W.H., Bickford, M.E., McLelland, J.M., Nagle, A.N., and Swarr, G.J., 2010, Mechanism of metamorphic zircon growth in a granulite-facies quartzite, Adirondack Highlands, Grenville Province, New York: American Mineralogist, v. 95, p. 1796–1806.

Prucha, J., 1957, Pyrite deposits of St. Lawrence and Jefferson Counties, New York: Albany, University of the State of New York, 87 p.

Regan, S., 2010, Magmatic evolution beneath ancestral Laurentia during Shawinigan orogenesis: Southern Grenville Province, Adirondacks [B.S. thesis]: Canton, New York, St. Lawrence University, 99 p.

Regen, S.P., Chiarenzelli, J.R., McLelland, J.M., and Cousens, B., 2011, Evidence for an enriched asthenospheric source for coronitic metagabbros in the Adirondack Highlands: Geosphere, doi:10.1130/GES00629.1 (in press).

Reitz, K., and Valentino, D., 2006, Structural analysis of a ductile shear zone at Wellesley Island, Thousand Islands, New York: Philadelphia, Pennsylvania, Geological Society of America Abstracts with Programs, Annual Meeting, v. 38, p. 67.

Revetta, F.A., and McDermott, A. M., 2003, The compilation and preparation of high-resolution gravity data for petroleum exploration in New York State and adjoining regions: New York State Energy Research Development Authority (NYSERDA) PON 715-02.

Rickard, L., Isachsen, Y.W., and Fisher, D.W., 1970, Adirondack Sheet: New York State Museum, Map and Chart Series 15, scale 1:250,000.

Rivers, T., 1997, Lithotectonic elements of the Grenville Province: Precambrian Research, v. 86, p. 117–154, doi: 10.1016/S0301-9268(97)00038-7.

Rivers, T., 2008, Assembly and preservation of lower, mid, and upper orogenic crust in the Grenville Province—Implications for the evolution of large hot long-duration orogens: Precambrian Research, v. 167, p. 237–259, doi: 10.1016/j.precamres.2008.08.005.

Rivers, T., and Corrigan, D., 2000, Convergent margin on southeastern Laurentia during the Mesoproterozoic: Tectonic implications: Canadian Journal of Earth Sciences, v. 37, p. 359–383, doi: 10.1139/cjes-37-2-3-359.

Rudnick, R.L., and Gao, S., (2003), Composition of the continental crust, *in* Rudnick, R.L., ed., The Crust: Volume 3: Elsevier, p. 1–64.

Sager-Kinsman, A.E., and Parrish, R.R., 1993, Geochronology of detrital zircons from the Elzevir and Frontenac terranes, Central Metasedimentary Belt, Grenville Province, Ontario: Canadian Journal of Earth Sciences, v. 30, p. 465–473, doi: 10.1139/e93-034.

Selleck, B.W., McLelland, J.M., and Bickford, M.E., 2005, Granite emplacement during tectonic exhumation: The Adirondack example: Geology, v. 33, p. 781–784, doi: 10.1130/G21631.1.

Smith, T.E., and Harris, M.J., 1996, The Queensborough mafic-ultramafic complex: A fragment of a Meso-Proterozoic ophiolite?: Grenville Province, Canada: Tectonophysics, v. 265, p. 53–82, doi: 10.1016/S0040-1951(96)00146-1.

Streckeisen, A.L., 1973, Plutonic rocks—Classification and nomenclature recommended by the International Union of the Geological Sciences Subcommission on the Systematics of Igneous Rocks: Geotimes, v. 18, no. 10, p. 26–30.

Streepey, M.M., Johnson, E., Mezger, K., and Van Der Pluijm, B.A., 2001, The early history of the Carthage-Colton shear zone, Grenville Province, New York: The Journal of Geology, v. 109, p. 479–492, doi: 10.1086/320792.

Sun, S.-s., and McDonough, W. F., 1989, Chemical and isotopic systematics of oceanic basalts: Implications for mantle composition and processes, *in* Saunders, A.D. and Norry, M.J., eds., Magmatism in the Ocean Basins: The Geological Society of London Special Publication 42, p. 313–345.

Tiedt, K., and Kelson, C., 2008, Geochemical and mineralogical characterization of ore from the Pyrites and Stella pyrite deposits, St. Lawrence County, New York: Geological Society of America Abstracts with Programs, v. 40, p. 6.

Tyler, R.D., 1979, Chloride metasomatism in the southern part of the Pierrepont quadrangle, Adirondack Mountains, New York [Ph.D. thesis]: Binghamton, New York, State University of New York.

Wasteneys, H., McLelland, J.M., and Lumbers, S., 1999, Precise zircon geochronology in the Adirondack Lowlands and implications for revising plate-tectonic models of the Central Metasedimentary Belt and Adirondack Mountains, Grenville Province, Ontario and New York: Canadian Journal of Earth Sciences, v. 36, p. 967–984, doi: 10.1139/cjes-36-6-967.

Wiener, R.W., 1983, Adirondack Highlands-Northwest Lowlands "boundary": A multiply folded intrusive contact with associated mylonitization: Geological Society of America Bulletin, v. 94, p. 1081–1108, doi: 10.1130/0016-7606(1983)94<1081:AHLBAM>2.0.CO;2.

Manuscript Received 3 May 2010
Revised Manuscript Received 17 October 2010
Manuscript Accepted 21 October 2010